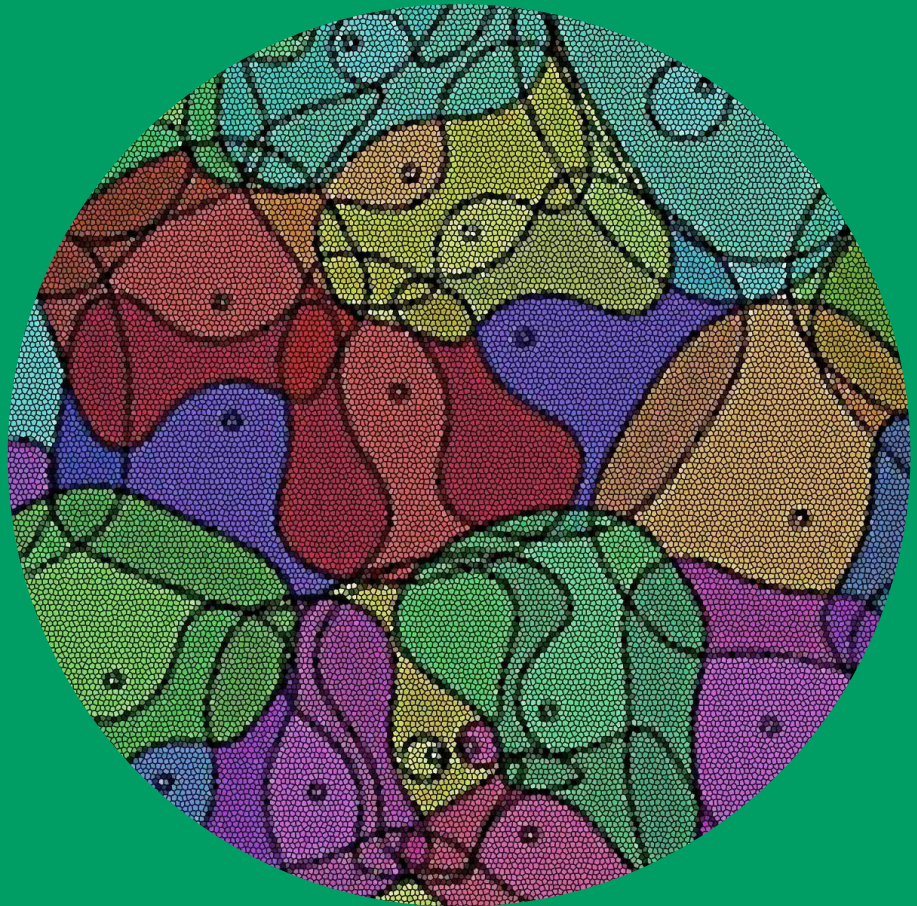


Probabilistic Cache Policy Design for Cellular Networks with Stochastic Geometry Analysis

Mohsen Amidzade



Probabilistic Cache Policy Design for Cellular Networks with Stochastic Geometry Analysis

Mohsen Amidzade

A doctoral thesis completed for the degree of Doctor of Science (Technology) to be defended, with the permission of the Aalto University School of Electrical Engineering, at a public examination held at the lecture hall Y203a Hall B located at Otakaari 1 on 22 January 2024 at 12 noon.

Aalto University
School of Electrical Engineering
Department of Information and Communications Engineering

Supervising professor

Professor Olav Tirkkonen, Aalto University, Finland

Thesis advisor

Doctor Hanan Al-Tous, Aalto University, Finland

Preliminary examiners

Professor Italo Atzeni, University of Oulu, Finland

Research Director, Bartłomiej Błaszczyszyn, INRIA/ENS, France

Opponents

Professor Di Yuan, Uppsala University, Sweden

Professor Italo Atzeni, University of Oulu, Finland

Aalto University publication series

DOCTORAL THESES 226/2023

© 2023 Mohsen Amidzade

ISBN 978-952-64-1600-7 (printed)

ISBN 978-952-64-1601-4 (pdf)

ISSN 1799-4934 (printed)

ISSN 1799-4942 (pdf)

<http://urn.fi/URN:ISBN:978-952-64-1601-4>

Unigrafia Oy

Helsinki 2023

Finland



Printed matter
4041-0619

Author

Mohsen Amidzade

Name of the doctoral thesis

Probabilistic Cache Policy Design for Cellular Networks with Stochastic Geometry Analysis

Publisher School of Electrical Engineering

Unit Department of Information and Communications Engineering

Series Aalto University publication series DOCTORAL THESES 226/2023

Field of research Caching for Cellular Wireless Networks

Manuscript submitted 4 December 2023

Date of the defence 22 January 2024

Permission for public defence granted (date) 27 October 2023

Language English

Monograph

Article thesis

Essay thesis

Abstract

The annual data traffic of mobile cellular networks is growing explosively, which has led to backhaul link congestion and latency during data reception from cellular networks. For the fifth generation (5G) of cellular systems, faster transmission speeds, lower latency, and higher spectral efficiency than the previous generations are required. Edge caching promisingly fulfills these requirements by alleviating the unprecedented data congestion and traffic escalation issues of cellular networks. Edge caching is a technique to proactively store the potentially preferable files at the edge of the network (e.g. base stations or user equipment). To achieve an appropriate cache strategy, the two phases of cache placement and cache delivery need to be addressed and optimized. Moreover, a cache policy can be designed based on a static or dynamic framework. For the former, only one shot of network operation is considered, while for the latter, the dynamics of network operation are taken into account.

This thesis aims to design optimal static and dynamic caching policies based on the considered model of network operation. For the static caching, this thesis considers the multipoint multicast transmission scheme with a probabilistic cache placement. Building on stochastic geometry, the outage probability is analyzed as network performance to design a static cache strategy. As such, a constrained optimization problem is formulated considering resource and cache allocation parameters, and two algorithms are devised to numerically solve it. Simulation results show that the usage of multipoint multicast is a promising and competitive approach compared to the single-point scheme from the literature. This thesis also proposes a hybrid scheme combining the multi-antenna single-point unicast and multipoint multicast components to simultaneously leverage the advantages of these schemes for a static cache strategy. To find the hybrid cache solution, a time-varying optimization problem is formulated considering cache and resource allocation parameters as well as content assignment between those two different components. Simulation results indicate the superiority of the proposed hybrid scheme from the spectral efficiency perspective. For the dynamic caching, the dynamics of the user requests in a cellular network are formulated based on a Markov decision process. As such, a reinforcement learning algorithm is exploited to devise a dynamic cache strategy. Simulation results show significant improvements brought by proposed dynamic caching from the quality-of-service and power consumption point-of-view.

Keywords Probabilistic cache policy, Distributed cache placement, Multipoint multicast transmission, Stochastic geometry

ISBN (printed) 978-952-64-1600-7

ISBN (pdf) 978-952-64-1601-4

ISSN (printed) 1799-4934

ISSN (pdf) 1799-4942

Location of publisher Helsinki

Location of printing Helsinki **Year** 2023

Pages 164

urn <http://urn.fi/URN:ISBN:978-952-64-1601-4>

Preface

The research related to this dissertation has been conducted in the Department of Communications and Networking (ComNet) of Aalto University. It provided me with an irreplaceable, inspiring, and comfortable workplace such that I enjoyed studying there for all the seconds I spent. As such, I am grateful for everything provided by Aalto ComNet, especially for its academic atmosphere and energetic environment.

Foremost, I would like to appreciate my supervisor Prof. Olav Tirkkonen, who patiently directed me through this research, gave me precious advice and guidelines, and helped me to enhance our scientific contributions.

Moreover, I sincerely thank Dr. Hanan Al-Tous for her help and cooperation in writing papers and scientific debate. My gratitude also goes to Prof. Giuseppe Caire for sharing his scientific thoughts with me to enrich this research.

Finally, I thank my wife and parents for all support and encouragement they provided me to finish my Ph.D. study.

Helsinki, December 4, 2023,

Mohsen Amidzade

Contents

Preface	1
Contents	3
List of Publications	7
Author's Contribution	9
List of Figures	11
Abbreviations	15
Symbols and Notations	17
1. Introduction	19
1.1 Motivation	19
1.2 Scope of the Thesis	22
1.3 Contributions and Structure of the Thesis	23
1.4 Summary of the Publications	24
1.5 Interconnection among Chapters, Publications, Models and Method	25
2. Background on the Analytical Tools	29
2.1 Stochastic Geometry	29
2.2 Parametric Optimization	31
2.3 Markov Decision Process, Reinforcement Learning, and A2C Algorithm	32
3. Cache Models and Methods	37
3.1 Cache Policy in Cellular Networks	37
3.2 System Model	45
3.3 Content Placement	45
3.4 Content Delivery and Multipoint Multicast Scheme	45
3.5 Signal Propagation and System Performance	46

4. Orthogonal Multipoint Multicast Cache Policy	49
4.1 Overall System Outage Probability	49
4.2 Resource and Cache Allocation Problem	50
4.3 Simulation Results	54
4.3.1 Threshold-Based OMPMC Scheme	54
4.3.2 Only Bandwidth-Optimized OMPMC Scheme	54
4.3.3 Single-Point Scheme from the Literature	55
4.3.4 Performance Results	55
4.4 Conclusion	56
5. Multipoint Multicast Caching With ICI and IBI	59
5.1 Overall System Outage Probability	59
5.2 Resource and Cache Allocation Problem	60
5.3 A prediction-correction Algorithm for Optimal Cache policy	62
5.4 Simulation Results	63
5.4.1 Threshold-based Solution	63
5.4.2 Interference-Ignoring Solution	63
5.4.3 Performance Results	63
5.5 Conclusion	66
6. Hybrid Cache-enabled Traffic Offloading with Single-point Unicast	67
6.1 Hybrid Delivery Scheme	67
6.2 Hybrid Outage Probability	68
6.3 Optimal Hybrid Cache Policy	70
6.4 Simulation Results	71
6.5 Conclusion	74
7. Dynamic Cache Policy Design using Reinforcement Learning	75
7.1 Timing Model of Network Operation	75
7.1.1 File Popularity and User Requests	76
7.1.2 Cache Placement	76
7.1.3 Cache Delivery	76
7.1.4 UE Cache Policy	77
7.1.5 Overall View of Network Operation	77
7.2 RL-based Dynamic Cache Policy	77
7.2.1 Problem Formulation	78
7.2.2 Structure of Actor and Critic Networks	80
7.2.3 RL-based Cache Policy Algorithm	80
7.3 Simulation Results	81
7.4 Conclusion	83
8. Conclusion and Future Work	85
References	87

Errata	93
Publications	95

List of Publications

This thesis consists of an overview and of the following publications which are referred to in the text by their Roman numerals.

- I** Mohsen Amidzadeh, Hanan Al-Tous, Olav Tirkkonen, Giuseppe Caire. Cellular Network Caching Based on Multipoint Multicast Transmissions. In *IEEE Global Communications Conference (GLOBECOM)*, Taipei, pp. 1-6, Dec. 2020.
- II** Mohsen Amidzadeh, Hanan Al-Tous, Olav Tirkkonen, Giuseppe Caire. Orthogonal Multipoint Multicast Caching in OFDM Cellular Networks with ICI and IBI. In *IEEE Annual International Symposium on Personal, Indoor and Mobile Radio Communications (PIMRC)*, Helsinki, pp. 394-399, Oct. 2021.
- III** Mohsen Amidzadeh, Hanan Al-Tous, Olav Tirkkonen, Giuseppe Caire. Cellular Traffic Offloading with Optimized Compound Single-point Unicast and Cache-based Multipoint Multicast. In *IEEE Wireless Communications and Networking Conference (WCNC)*, Austin, pp. 2268-2273, May. 2022.
- IV** Mohsen Amidzadeh, Hanan Al-Tous, Olav Tirkkonen, Junshan Zhang. Joint Cache Placement and Delivery Design using Reinforcement Learning for Cellular Networks. In *IEEE Vehicular Technology Conference (VTC)*, Helsinki, pp. 1-6, Jun. 2021.
- V** Mohsen Amidzadeh, Hanan Al-Tous, Olav Tirkkonen, Giuseppe Caire. Caching in Cellular Networks Based on Multipoint Multicast Transmissions. In *IEEE Transactions on Wireless Communications*, pp. 2393 - 2408, Oct. 2022.
- VI** Mohsen Amidzadeh, Hanan Al-Tous, Olav Tirkkonen, Giuseppe Caire. Multipoint Multicast Caching in the Presence of Multipoint and Multipath Interference via an Optimized Parametric Programming. *Submitted to a Journal*, Dec. 2022.

Author's Contribution

Publication I: “Cellular Network Caching Based on Multipoint Multicast Transmissions”

The author had a partial responsibility in formulating the ideas, and main responsibility for mathematical derivations, producing numerical results as well as writing the article.

Publication II: “Orthogonal Multipoint Multicast Caching in OFDM Cellular Networks with ICI and IBI”

The author had a partial responsibility in formulating the ideas, and main responsibility for mathematical derivations, producing numerical results as well as writing the article.

Publication III: “Cellular Traffic Offloading with Optimized Compound Single-point Unicast and Cache-based Multipoint Multicast”

The author had main responsibility in formulating the ideas, producing numerical results and writing the article.

Publication IV: “Joint Cache Placement and Delivery Design using Reinforcement Learning for Cellular Networks”

The author had main responsibility in formulating the idea, producing numerical results as well as writing the article.

Publication V: “Caching in Cellular Networks Based on Multipoint Multicast Transmissions”

The author had a partial responsibility in formulating the ideas, and main responsibility for mathematical derivations, producing numerical results as well as writing the article.

Publication VI: “Multipoint Multicast Caching in the Presence of Multipoint and Multipath Interference via an Optimized Parametric Programming”

The author had a partial responsibility in formulating the ideas, and main responsibility for mathematical derivations, producing numerical results as well as writing the article.

Language check

The language of my dissertation has been checked by Prof. Olav Tirkkonen. I have personally examined and accepted/rejected the results of the language check one by one. This has not affected the scientific content of my dissertation.

List of Figures

1.1	Interconnection between chapters/publications and problem formulations/solution approaches	28
2.1	The diagram of A2C algorithm. The red arrows show the update processes of actor and critic networks.	34
3.1	Example of a user-centric SPUC networking	38
3.2	Example of an SPMC networking	41
3.3	Example of an MPUC networking	42
3.4	Example of an information-centric MPMC networking	44
4.1	The overall outage probability as a function of cache intensity for skewness $\tau = 2.6$, $N = 200$ and $M = 20$	57
4.2	The overall outage probability as a function of cache intensity for skewness $\tau = 0.8$, $N = 200$ and $M = 20$	57
4.3	The bandwidth allocation as a function of file index for cache intensity $\lambda = 30$ and skewness $\tau = 2.6$	58
5.1	The overall outage probability as a function of ratio of CP length to the symbol length for skewness $\tau = 2.6$ and effective intensity $\lambda_{\text{eff}} = 3 \times 10^3$	64
5.2	The overall outage probability as a function of the effective intensity λ_{eff} for skewness $\tau = 2.6$, and relative CP length 7%.	64
5.3	The overall outage probability as a function of ratio of CP length to the symbol length for skewness $\tau = 0.6$ and effective intensity $\lambda_{\text{eff}} = 4 \times 10^3$	65
6.1	The total outage probability as a function of the UE intensity λ_{UE}	72
6.2	The resource allocation ratio as a function of the UE intensity λ_{UE}	73

6.3	The file classification ratio as a function of the UE intensity λ_{UE}	73
7.1	The interactions between UEs, BSs and core network for CPD policy. Phase (a): UEs requests. Phase (b): BSs fetch files from the core network and update their caches. Phase (c): OMPMC cache delivery and update of UEs caches.	78
7.2	The structure of the actor neural network $\pi_{\theta}(\cdot)$	80
7.3	Training performance of the RL agent in term of the accumulative reward.	82
7.4	Performance comparison between the RL-based CPD, LFU, LRU and " <i>Optimum</i> " cache policies in term of the accumulative reward.	83
7.5	Experimental CDF of the QoS reward during network dynamics.	84
7.6	Experimental CDF of the backhaul reward during network dynamics.	84

List of Tables

1.1	Model assumptions used in the chapters and publications.	27
4.1	Cache Policy Approaches	55

Abbreviations

3GPP	3rd Generation Partnership Project
A2C	Advantageous Actor-Critic
AWGN	Additive White Gaussian Noise
BS	Base Station
CDF	Cumulative Density Function
CP	Cyclic Prefix
CPD	Cache Placement and Delivery
CSI	Channel Side Information
GHG	Greenhouse Gas
GPS	Global Positioning System
HetNet	Heterogeneous Network
IBI	Inter-Block Interference
ICI	Inter-Carrier Interference
ICT	Information and Communication Technology
ICN	Information-Centric Network
LFU	Least Frequently Used
LRU	Least Recently Used
LTE	Long-Term Evolution
MBMS	Multimedia Broadcast Multicast Service
MDP	Markov Decision Process

Abbreviations

MDS Minimum Distance Separable

MPMC Multipoint Multicast

MPUC Multipoint Unicast

NLOS No line-of-Sight

NN Neural Network

ODE Ordinary Differential Equation

OFDM Orthogonal Frequency-Division Multiplexing

OMPMC Orthogonal Multipoint Multicast

PCM prediction-correction Method

PDF Probability Density Function

PPP Poisson Point Process

QoS Quality of Service

RL Reinforcement Learning

SFN Single-Frequency Network

SINR Signal-to-Interference-plus-Noise Ratio

SNR Signal-to-Noise Ratio

SPMC Single-Point Multicast

SPUC Single-Point Unicast

UE User Equipment

Symbols and Notations

$\mathbf{0}$ is a vector with all elements equal to zero.

$\mathbf{1}$ is a vector with all elements equal to one.

$\delta_{nm} = \begin{cases} 1 & n = m \\ 0 & n \neq m \end{cases}$ is the Kronecher delta function.

$\log(a) = \log_e(a)$ is the natural logarithm of the number a with e being the Napier's constant.

$\dot{g}(t) = \frac{dg(t)}{dt}$ is the derivative of function $g(t)$ with respect to t .

$D_z h(z) = \frac{dh(z)}{dz}$ is the derivative of function $h(z)$ with respect to z .

$D_z^2 h(z) = \frac{d^2 h(z)}{dz^2}$ is the second derivative of function $h(z)$ with respect to z .

$D_{z,w} h(z,w) = \frac{d^2 h(z,w)}{dz dw}$ is the derivative of function $h(z,w)$ with respect to z and w .

$\nabla f(\mathbf{x}) = \left(\frac{df(\mathbf{x})}{dx_1} \quad \dots \quad \frac{df(\mathbf{x})}{dx_n} \right)^\top$ is the gradient vector of multivariate function $f(\cdot)$ with respect to vector $\mathbf{x} = [x_1, \dots, x_n]^\top$.

$\nabla^2 f(\mathbf{x}) = \begin{pmatrix} \frac{d^2 f(\mathbf{x})}{dx_1^2} & \dots & \frac{d^2 f(\mathbf{x})}{dx_1 dx_n} \\ \dots & \dots & \dots \\ \frac{d^2 f(\mathbf{x})}{dx_n dx_1} & \dots & \frac{d^2 f(\mathbf{x})}{dx_n^2} \end{pmatrix}$ is the Hessian matrix of multivariate function $f(\cdot)$ with respect to vector $\mathbf{x} = [x_1, \dots, x_n]^\top$.

$\|\mathbf{x}\|_2 = \mathbf{x}^\top \mathbf{x} = \sum_{i=1}^n x_i^2$ is the Euclidean norm of vector \mathbf{x} .

$\operatorname{erfc}(x) = \frac{2}{\sqrt{\pi}} \int_x^\infty \exp(-t^2) dt$ is the complementary error function.

$B(n, m) = \int_0^1 t^{n-1} (1-t)^{m-1} dt$ is the Beta function.

$(a)_n = \begin{cases} 1 & n = 0 \\ a(a+1)\dots(a+n-1) & n > 0 \end{cases}$ is Pochhammer symbol.

${}_2F_1(a, b, c, z) = \sum_{n=0}^{\infty} \frac{(a)_n (b)_n}{(c)_n} \frac{z^n}{n!}$ is the Gaussian hypergeometric function.

$P_Y(\cdot) = \mathbf{Pr}(Y \leq y)$ is the probability density function (PDF) of the continuous random variable Y . For simplicity, we might show it by $P(y)$.

$\mathbb{E}_Y\{f(y)\} = \int_{\mathcal{Y}} f(y)P_Y(y)dy$ is the expectation of function $f(y)$ with y being drawn from $P_Y(\cdot)$, where \mathcal{Y} is the support set of $P_Y(\cdot)$. For the simplicity, we might show it by $\mathbb{E}\{f(y)\}$.

$H(P_X(\cdot)) = \int_{\mathcal{X}} P_X(x) \log P_X(x) dx$ is the differential entropy of PDF $P_X(\cdot)$, where \mathcal{X} is the support set of $P_X(\cdot)$.

\odot is the Hadamard product which for vectors $\mathbf{a} = [a_1, \dots, a_n]^\top$ and $\mathbf{b} = [b_1, \dots, b_n]^\top$, we have: $\mathbf{a} \odot \mathbf{b} = [a_1 b_1, \dots, a_n b_n]^\top$.

$\text{Dirichlet}(\mathbf{x}, \mathbf{a})$ is the Dirichlet distribution evaluated at vector $\mathbf{x} = [x_1, \dots, x_n]^\top$, which is a multivariate PDF. This PDF is characterized by the concentrate vector $\mathbf{a} = [a_1, \dots, a_n]^\top$ with $a_i \geq 0$. The support set of this PDF is found by: $\{\mathbf{x} \in \mathbb{R}^n \mid 0 \leq x_i \leq 1, \sum_{i=1}^n x_i = 1\}$. For the simplicity, we might show it by $\text{Dirichlet}(\mathbf{a})$.

1. Introduction

1.1 Motivation

The annual data traffic of mobile cellular networks grows explosively between 25% and 60% [54,77], posing a challenge for current and upcoming networks [10]. This problem leads to congestion and latency during data reception from cellular networks. Additionally, the energy consumption of Information and Communications Technology (ICT) is between 2% and 10% of the whole energy consumption [26, 48], which has a significant effect on global warming through Greenhouse Gas (GHG) emissions [55]. Approximately one third of this energy consumption is related to the mobile wireless networks [26]. In the domain of the fifth generation (5G) of cellular systems, faster transmission speeds, lower latency, and higher spectral efficiency than the previous generations are required. For this generation, the target peak data rates and spectral efficiency are set to 10 Gb/s and 30 bps/Hz, respectively for the downlink, and 20 Gb/s and 15 bps/Hz for the uplink. [2]. To meet these requirements and to cope with the aforementioned problems, wireless caching or edge caching (referred to simply as caching) has been proposed as a promising technology [10,41]. As such, caching holds great potential to alleviate backhaul link congestions, improve the energy efficiency, and reduce traffic latency.

Stochastic geometry is leveraged as an analytical tool to model and analyze the performance metrics of cellular networks [7–9, 33]. It provides a spatial distribution to model the location of users and deployment of cache-equipped edges. This probabilistic methodology makes the network performance metrics tractable for analyzing and policy optimization, and as such facilitates the process of optimizing the network parameters.

To properly address the problem of caching in cellular networks, *cache placement* and *cache delivery* need to be considered [10, 41]. Cache placement is designed based on either probabilistic or deterministic methods. A comparison between these two placement approaches is as follows.

- Probabilistic cache placement can be formulated based on a file-specific distribution function [14, 30, 59, 60], which determines the probability that a file should be placed at the cache-equipped nodes. This Probabilistic approach enables the usage of stochastic geometry to design a cache policy. More specifically, the deployment of cache-equipped nodes and users can be modelled by independent Poisson point processes (PPPs). Stochastic geometry not only simplifies cache policy optimization due to the resulting tractable performance metrics, but it also empowers us to analyze the policy in the network level rather than in a user-specific manner. As a result, a consistent probabilistic model is achieved which allows us to analyze the cache policy in the network level and with network-wide parameters. This approach is scalable and can be applied to large networks. In contrast, for the deterministic method, one has to deal with user-specific discrete variables [53, 63], which makes it hard to optimize the cache policy for large networks. Furthermore, analyzing the cache policy using stochastic geometry becomes extremely intricate in this case.
- In contrast to the deterministic approach, the probabilistic one can lead to a decentralized cache placement strategy. More specifically, the solution of probabilistic approach provides a common distribution function by which each cache-equipped node can store files independent of other nodes. Hence, caching nodes independently and randomly store contents based on an optimized distribution function.

Considering these advantages of a probabilistic approach over a deterministic one, we concentrate on the former in this thesis.

Regarding the cache delivery phase, it is important to differentiate between different transmission schemes. Considering whether one or many users are served with a transmission, and further, whether one or multiple Base Stations (BSs) participates in a transmission, we get four essential methods: Single-Point Unicast (SPUC) [21, 71, 73, 78], Single-Point Multicast (SPMC) [20, 53, 75], Multipoint Unicast (MPUC) [63], and Multipoint Multicast (MPMC). They are briefly explained as follows.

- SPUC is an on-demand delivery approach implemented in cellular networks as the conventional content transmission scheme. It connects each requesting user to a BS in order to be individually served. Transmission from one BS to multiple users does not happen in the same time-frequency resource, but it is performed using a multiple access technique. Considering that SPUC satisfies users by an on-demand individual transmission scheme, it constitutes an example of user-centric networking. However, SPUC can lead to frequent information passage from content providers to the network edge, especially when the network has users with the same request. Not to mention that transmission

between a serving BS and a requesting user suffers from co-channel interference due to transmission of other BSs.

- In SPMC, each BS multicasts content toward multiple users in the same time-frequency resource. However, each user is only served by one BS. In contrast to SPUC, each BS may respond to multiple requests at once. Hence, SPMC can be considered as connection-centric networking. As SPUC, this scheme also suffers from co-channel interference.
- In MPUC, each user can be served by multiple BSs in the same time-frequency resource. However, simultaneous transmissions to multiple users in the same time-frequency resource do not happen. Transmission from one BS to multiple users is performed using a multiple access technique.
- In MPMC, each user can be served by multiple BSs and each BS might participate in multicast transmissions toward multiple users in the same time-frequency resource. In this scheme, users with the same request can be responded, at once, by a network-wide transmission based on a cooperation of multiple BSs. This makes MPMC more spectrally efficient as compared to single-point transmission schemes. This scheme thus constitutes information-centric networking, as it leverages a location-independent content-specific broadcast to satisfy the file requests. In addition, if MPMC applies an orthogonal resource allocation for transmitting different files, co-channel interference can be considerably mitigated.

In this dissertation, we focus on the MPMC cache policy due to the following reasons:

- MPMC has not been extensively studied and analyzed in the context of wireless caching policies.
- MPMC scheme does not suffer heavily from co-channel interference, unlike SPUC and SPMC.
- In a situation of cellular network with users requesting popular contents, the advantage of MPMC against other delivery schemes is considerable, as this scheme can be applied to transmit popular files across to the whole network, in the same time-frequency resource, to satisfy all UEs being interested in those files. As such, it can avoid redundant information flow from content providers to the network edge.

Here, it is noteworthy to mention the usage of multipoint multicast in wireless systems. Multipoint broadcast transmissions are applied in digital terrestrial TV broadcasting systems [58], while MPMC content delivery has been applied in Long-Term Evolution (LTE) systems in the context of enhanced MBMS [47, 68]. In a multi-cell transmission mode, all serving

BSs broadcast the same file into the air in a Single-Frequency-Network (SFN) configuration. As such, the file is concurrently transmitted over the same bandwidth within the whole network. A non-SFN MPMC scheme has been considered together with coded caching at the user end in [12]. In this scheme, the only collaboration between BSs comes from the Minimum Distance Separable (MDS) coding, and the BSs are not equipped with caches. In contrast to [12], we consider that caching also happens at the edge of the network, not merely at the UEs. We also assume that a UE cannot separate signals from different BSs while it decodes its requested signal based on an aggregated signal from all caching BSs.

Motivated by the advantages of probabilistic cache placement approaches and multipoint multicast cache delivery scheme, this thesis studies the cache policy optimization for edge cache-enabled cellular networks from the spectral efficiency and traffic reduction perspectives.

1.2 Scope of the Thesis

The main objective of this thesis is to study wireless caching for cellular networks from the spectral-efficiency perspective. As such, we investigate the *cache placement* and *cache delivery* as two phases of wireless caching. We mostly use the overall outage probability, defined as *the probability that a typical mobile user cannot successfully receive its requested file*, as an efficiency metric for cellular networks. More specifically, we investigate how the files should be proactively cached at the edge of the network, and how the cached files should be transmitted to requesting users, such that the overall outage probability of the cellular network is minimized.

We use stochastic geometry as one of the main analytical tools throughout this dissertation. It provides us a stochastic spatial framework based on that we can analytically obtain tractable performance metrics for proposed cache policy and optimize it.

We consider a scenario where the files are stored at the edge of the network based on a probabilistic cache placement strategy. For this, a network-wide probability distribution is considered for the cache-equipped BSs to store the files. For the cache delivery, we apply a multicast transmission scheme with a network-wide file-specific resource allocation strategy. In the multicast scheme, the files are simultaneously broadcasted towards the users in disjoint resources. As such, we jointly optimize the aforementioned probabilistic cache placement and resource allocation of the multicast delivery scheme to design an optimum cache policy.

We further consider a hybrid delivery scheme combining the multicast and unicast transmission schemes and classify the files into two sets to decide which set should be served by which transmission scheme. We then jointly optimize the hybrid scheme and the classification to design an

optimum cache strategy from the spectral efficiency perspective.

We also go beyond the static cache delivery, by considering the dynamics of the network operation over time. As such, we use Markov Decision Process (MDP) to model the network dynamics and use a Reinforcement Learning (RL) algorithm to design an optimum dynamic cache policy.

1.3 Contributions and Structure of the Thesis

This thesis is devoted to studying wireless caching for cellular networks from the spectral efficiency perspective. System models, methodology, mathematical analysis, and numerical simulations and results are provided for wireless caching. The cache policy optimization is based on considering spectral efficiency, Quality-of-Service (QoS), and backhaul load of cellular networks. The results of this dissertation can be applied to design more spectral-efficient wireless networks.

The remainder of this thesis is organized as follows. In Chapter 2, we introduce some mathematical background needed for the main part of the work. This background encompasses both the formulation approach and the solution approach. The former includes *stochastic geometry*, *parametric optimization*, *policy distribution optimization* and *Markov decision process*, and the latter includes *prediction-correction method*, *reinforcement learning* and *A2C algorithm*.

In Chapter 3, the system models and methodology for the applied cache policy design are explained. More specifically, the cache placement and delivery policies, network architectures and operations, interference and path-loss models, in the line with our study, are discussed.

In Chapters 4 and 5, we take into account a probabilistic cache placement and multipoint multicast cache delivery. An optimal cache policy is analyzed by modeling the network using stochastic geometry. As analytic results of these chapters, we derive expressions for the outage probability as a network performance metric. We thus optimize the cache policy considering the file-specific resource allocation of cache delivery and the content assignment of cache placement. In Chapter 4, the cache policy is analyzed for an OFDM-based transmission with an infinite CP length and as such co-channel interference can be ignored. However, in Chapter 5, co-channel interference arising from finite CP length is considered, based on which a cache policy is analyzed. Therefore, the cache policy presented in 5 stands for a more realistic propagation environment.

In Chapter 6, we take into account a hybrid cache delivery, compounding the multipoint multicast and single-point unicast transmission schemes. Inspired by the results of Chapters 4 and 5, which indicate that an optimal multipoint multicast policy only caches the most popular files, we classify the contents into two sets, and optimally decide which files should be

served by which transmission scheme. We then design a hybrid cache policy from the spectral-efficiency perspective, by optimizing the network-wide resource allocations, cache placement, and content classification.

In Chapters 4, 5 and 6, one-shot optimization is considered to design a cache policy, which can be considered to represent a static cache strategy. In Chapter 7, time-varying dynamics of the file popularity is considered and network operation is modeled based on an MDP. Considering that the popularity dynamics is unknown for the network, we use an RL algorithm to design a dynamic cache policy. Notice that in contrast to the model-based optimization techniques for which the system dynamics is a priori known, the RL algorithm can obtain the optimum solution without knowledge of the system dynamics. In fact, it implicitly estimates this dynamics merely by continually interacting with the environment.

Finally, we conclude this dissertation in Chapter 8 and give some directions for future work.

1.4 Summary of the Publications

This thesis has been based on six original publications, P-I, P-II, P-III, P-IV, P-V, and P-VI. The cache placement and delivery policy has been designed in these publications, considering the spectral efficiency perspective of cellular networks. In publication P-IV, we optimize a dynamic cache policy, in contrast to the Publications P-I, P-II, P-III, P-V, and P-VI, where a static cache strategy is designed.

In Publication P-I, we consider probabilistic cache placement with orthogonal multipoint multicast (OMPMC) cache delivery for cellular systems applying a SFN configuration. In this publication, we ignore the effect of co-channel interference caused by multipoint transmissions. We formulate the problem of finding the optimal cache policy as a constrained optimization problem jointly optimizing the resource allocation of multicast transmission and cache probability assignment of cache placement. We use a convex relaxation to obtain a low-complexity sub-optimal solution. This solution leads to a cache policy for the multipoint multicast scheme.

In Publication P-II, we extend the system model of Publication P-I to a more realistic case where co-channel interference is taken into account. Finding an optimal interference-aware cache policy is formulated based on a constrained optimization problem jointly optimizing the resource allocation and cache probability assignment. Since the objective of the formulated optimization problem lacks a closed-form expression, the methodology applied in Publication P-I can no longer be used. We thus use a sequential-based prediction-correction method to find the solution. This solution leads to an interference-aware cache policy for the multipoint multicast scheme.

Publication P-III considers a hybrid delivery scheme, comprising OMPMC service together with the conventional single-point unicast service, to design a cache policy. In order for these services to cooperate, the files are classified into two sets, where each set is supposed to be served by one transmission service. The cache policy design is thus formulated as a mixed-integer constrained optimization problem, jointly optimizing the resource allocation and cache probability assignment as well as the file classifier index. A sequential prediction-correction approach is used to find the solution to this problem, which provides an optimal cache policy for the hybrid transmission scheme.

In Publication P-IV, we design a dynamic cache policy by considering the timing model of network operation. The problem is formulated based on a MDP. We then use an RL algorithm, to design a dynamic cache policy for cellular networks configured based on the OMPMC transmission scheme.

Publication P-V extends the results and work of Publication P-I, by analyzing the outage probability in a more generic form, devising two algorithms to find the OMPMC cache policy, and giving more simulation results to confirm the superiority of the OMPMC scheme against other cache delivery approaches.

In Publication P-VI, we enrich the system model of Publication P-II to analyze the impact of multipath channel on the optimal multicast cache policy. The performance expressions are generalized based on the modified system model. Regarding the methodology for the optimal cache policy, a parametric programming is formulated based on some parametric functions. We then analyze the effect of the parametric function on the optimal cache policy and jointly find the numerical solution and optimal parametric functions with the aid of the calculus of variations.

1.5 Interconnection among Chapters, Publications, Models and Method

Table 1.1 illustrates the correspondence between chapters/publications and the model assumptions employed in this dissertation. In all chapters/publications, a probabilistic cache placement strategy is utilized for cache-equipped BSs. In addition to BS-caching, P-IV employs a caching model for requesting UEs, implemented by the probabilistic approach. This specific scenario is considered in Chapter 7. The content-centric OMPMC scheme is leveraged across all contributions. In P-III, a hybrid network that combines OMPMC and UE-centric SPUC schemes is utilized, and this hybrid scheme is discussed in Chapter 6. Throughout the contributions, the network operation is considered stationary, leading to a static cache policy. The exception to this is P-IV, where the dynamics of network operation are modeled using a Markov Decision Process (MDP), with a specific

focus on achieving a dynamic cache solution.

The transmission scheme predominantly employed in this thesis is OFDM. For P-I, P-III, P-IV, and P-V, an OFDM system with a long cyclic prefix (CP) is used, such that Inter-Block and Inter-Carrier Interference are not a problem. However, for P-II and P-VI, a practical OFDM system with a conventional CP length is employed. With a practical CP length, IBI and ICI cause co-channel interference at the receivers. In P-II, this interference is caused by multi-point transmission of OMPMC, whereas in P-VI, it arises from both multi-point transmission of OMPMC and a multi-path channel.

For all chapters/publications, a standard distance-dependent path-loss model is employed. In P-I, P-II, P-III, and P-IV, the analysis is conducted specifically for a path-loss exponent of four. However, for P-V and P-VI, as well as P-III and P-IV, the analysis encompasses all path-loss exponents greater than two.

Figure 1.1 depicts the relationship between chapters/publications and the problem formulations and solution approaches in this thesis. In Chapter 4, the cache policy problem is formulated as a constrained optimization problem. Subsequently, the cache strategies in P-I and P-V are designed through analysis of Karush-Kuhn-Tucker (KKT) conditions, convex relaxation, and relaxation gap analysis. In Chapters 5 and 6, the cache strategy problem is formulated as a parametric optimization problem. The cache policies in P-II, P-III, and P-VI are then devised using KKT-conditions analysis and prediction-correction methods. In Chapter 7, the dynamic cache policy is formulated using the concept of Markov Decision Process and policy distribution optimization. The cache policy in P-IV is optimized using a reinforcement learning algorithm, specifically the Advantage Actor-Critic (A2C) algorithm.

It is worth noting that stochastic geometry is widely employed in almost all contributions for the deployment model. Additionally, Campbell's theorem is utilized to accomplish the objectives of the corresponding optimization problems.

Table 1.1. Model assumptions used in the chapters and publications.

Publication / Chapter	Cache Placement	Cache Delivery	Network Architecture	Transmission Scheme	Network Operation	Interference Model	Path-loss Model
P-I / CH4	Probabilistic approach	OMPMC	Content-centric	OFDM with long CP length	Stationary	Ignored	Standard distance-dependent with path-loss exponent $\beta = 4$
P-II / CH5	Probabilistic approach	OMPMC	Content-centric	OFDM with practical CP length	Stationary	Co-channel interference caused by multipoint transmission	Standard distance-dependent with path-loss exponent $\beta = 4$
P-III / CH6	Probabilistic approach	Hybrid: OMPMC and beamforming SPUC, with disjoint resources	Content-centric and user-centric	OFDM with long CP length	Stationary	Ignored for OMPMC, inter-cell co-channel interference for SPUC	Standard distance dependent with path-loss exponent $\beta = 4$
P-IV / CH7	Probabilistic approach for BSs and UEs	OMPMC	Content-centric	OFDM with long CP length	Dynamic	Ignored	Standard distance dependent with path-loss exponent $\beta = 4$
P-V / CH4	Probabilistic approach	OMPMC	Content-centric	OFDM with long CP length	Stationary	Ignored	Standard distance dependent with path-loss exponent $\beta > 2$
P-VI / CH5	Probabilistic approach	OMPMC	Content-centric	OFDM with practical CP length	Stationary	Co-channel interference caused by multipath channel and multipoint transmission	Standard distance dependent with path-loss exponent $\beta > 2$

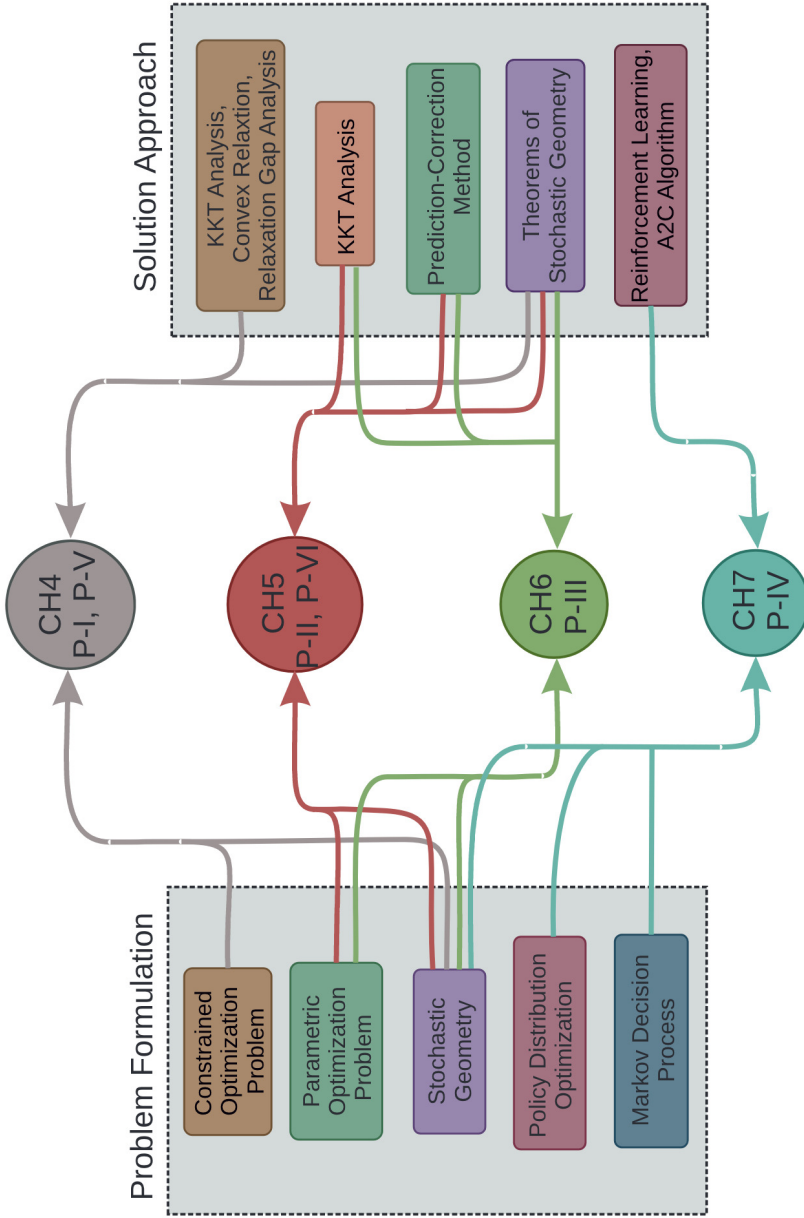


Figure 1.1. Interconnection between chapters/publications and problem formulations/solution approaches

2. Background on the Analytical Tools

In this chapter, we explain the background and main approaches leveraged for the analysis of this thesis. In this regard, we first explain the notion of stochastic geometry in Section 2.1 and address some of corresponding properties and theorems leveraged throughout this dissertation. We then discuss parametric optimization problems in Section 2.2 and explain the predictor-corrector method as a solution approach for that. At the end, we introduce the concept of MDP in Section 2.3 and describe the A2C algorithm as an approach for MDP problems.

2.1 Stochastic Geometry

Stochastic geometry studies the statistical specifications and behavior of random collections of points. A process creating random collections of points is called a point process, and the components of such a process are called points of the process. Each point is conventionally associated with a location-denoting vector $\mathbf{r} \in \mathbb{R}^m$ placed in a m -dimensional space. In this thesis, we are interested in the spatial Poisson Point Process (PPP) defined in Euclidean space. As its name suggests, this process is modeled based on the Poisson distribution. A homogeneous PPP Φ is characterized by two basic properties as follows [23]:

- Considering a bounded region of space A , and the number of points lying in this region $N(A)$, then $N(A)$ is a random variable possessing the Poisson distribution for which:

$$\Pr(N(A) = n) = e^{-\lambda|A|} \frac{(\lambda|A|)^n}{n!},$$

where λ is the intensity of process Φ indicating the mean number of points per unit space, and $|A|$ is the area of the region A .

- The number of points of Φ in k disjoint regions $\{A_i\}_{i=1}^k$ are characterized by k independent random variables $\{N(A_i)\}_{i=1}^k$. As such, one can

evaluate the following joint probability mass function:

$$\Pr\left(N(A_1) = n_1, \dots, N(A_k) = n_k\right) = \prod_{i=1}^k e^{-\lambda|A_i|} \frac{(\lambda|A_i|)^{n_i}}{n_i!}.$$

We further mention a useful theorem for PPPs, namely **Campbell's Theorem** [36], which is exploited throughout this thesis to analyze network performance metrics. This theorem states that for a PPP Φ , a function $f(\cdot) : \mathbb{R}^m \rightarrow \mathbb{R}$, and a random variable $\Sigma = \sum_{\mathbf{r}_i \in \Phi} f(\mathbf{r}_i)$, we have:

$$\mathbb{E}\{\Sigma\} = \lambda \int_{\mathbb{R}^m} f(\mathbf{x}) d\mathbf{x}.$$

Based on this theorem for the random variable $\Pi = \prod_{\mathbf{r}_i \in \Phi} f(\mathbf{r}_i)$, it can be derived that:

$$\mathbb{E}\{\Pi\} = \exp\left(\lambda \int_{\mathbb{R}^m} (f(\mathbf{x}) - 1) d\mathbf{x}\right).$$

We also use the **thinning property** of PPP throughout this thesis. Accordingly, if we mark the points of a λ -characterized PPP Φ with probability p , then the marked points constitute another PPP with intensity $p\lambda$, and the un-marked points another PPP with intensity $(1-p)\lambda$.

We also apply the **Slivnyak-Mecke Theorem** [8] in our stochastic geometry-based performance analysis. According to this theorem, for homogeneous PPPs, we can consider a point located at the origin of space, compute the performance for that point and then generalize the obtained result into the other points of the process.

Stochastic geometry is considered a versatile tool for modeling and analyzing wireless cellular networks, both for homogeneous and Het-Nets [6–9, 25, 33, 35]. In the context of caching at the wireless edge, Poisson Point Processes (PPP) have been used to model deployment of BSs and locations of UE in [21, 39, 70, 72, 75]. In [39], where BSs apply a beamforming content delivery and the expected ergodic spectral efficiency is optimized, stochastic geometry is used to model BS deployment. In [59], optimum cache policies are found in HetNets modelled based on independent PPPs. In [70], two independent PPPs are exploited to model the deployment of two tiers of a HetNets. Aiming to find an optimal cache placement policy, independent PPPs are exploited in [75] to obtain an expression for the successful transmission probability in a HetNet. In [72], the coverage probability is approximated using PPP for the multi-antenna small-cell networks to design an optimal cache placement policy. In [21], the authors leverage PPP to optimize the minimum of the cache hit rates of different request-related categorized UEs.

2.2 Parametric Optimization

A parametric optimization problem can be considered as a continuously varying problem when the objective function, the constraints, or both change continuously in time t [38, 61]. In this thesis, we are interested in a specific class of parametric optimization problem of the form:

$$P_0(t): \quad \min_{\{\mathbf{x}_n\}_{n=1}^N} \sum_{n=1}^N a_n(t) f_n(\mathbf{x}_n)$$

$$\text{s.t.} \quad \sum_{n=1}^N \mathbf{A}_n \mathbf{x}_n = \mathbf{l},$$

where $f_n(\cdot): \mathbb{R}^m \rightarrow \mathbb{R}$ is a scalar-valued function, $\mathbf{x}_n \in \mathbb{R}^m$ is the optimization variable, \mathbf{A}_n is a $m \times m$ matrix, and \mathbf{l} is a m -dimensional vector. We are interested in a sequential approach to find the optimal solution $\mathbf{x}_n^*(t)$ of $P_0(t)$, as a function of t . As such, we intend to extrapolate from a known optimal solution to other solutions of interest. We follow an approach along the lines of the homotopy continuation method [4]. By evaluating the Karush-Kuhn-Tucker (KKT) conditions of $P_0(t)$ [15] and following the homotopy continuation method, we get the Ordinary Differential Equation (ODE) associated with $P_0(t)$:

$$\dot{\mathbf{x}}_n(t) = (a_n(t) \nabla^2 f_n(\mathbf{x}_n))^{-1} (\mathbf{A}_n^\top \mathbf{d}_1 - \dot{a}_n(t) \nabla f_n(\mathbf{x}_n)), \quad n = 1, \dots, N, \quad (2.1)$$

where

$$\mathbf{d}_1 = \left(\sum_{n=1}^N \mathbf{A}_n (a_n(t) \nabla^2 f_n(\mathbf{x}_n))^{-1} \mathbf{A}_n^\top \right)^{-1} \sum_{n=1}^N \frac{\dot{a}_n(t)}{a_n(t)} \mathbf{A}_n \nabla^2 f_n(\mathbf{x}_n)^{-1} \nabla f_n(\mathbf{x}_n).$$

By solving the ODEs (2.1) for a initial point $t = t_0$ and a point of interest $t = t_e$, the optimal solution of $P_0(t_e)$ can be found, assuming the existence of $\nabla f_n(\mathbf{x}_n)^{-1}$ and $\left(\sum_{n=1}^N \mathbf{A}_n (a_n(t) \nabla f_n(\mathbf{x}_n))^{-1} \right)^{-1}$ for $t \in [t_0, t_e]$.

To solve (2.1), it is conventional to exploit the prediction-correction method [5, 27, 51], as a numerical tracking approach. This method includes the predictor and corrector steps, where in the predictor step the solution trajectory is traced based on the evolution of the objective function in time, and in the correction step the predicted solution is adjusted using a Newton-based directional method [61].

For this approach, incremental steps Δt are considered, by which (2.1) is linearized to give the *predictor step*:

$$\mathbf{x}_n(t + \Delta t) = \mathbf{x}_n(t) + \dot{\mathbf{x}}_n(t) \Delta t. \quad (2.2)$$

We thus start from the given solution $\mathbf{x}_n(t_0)$, obtain $\dot{\mathbf{x}}_n(t_0)$ from (2.1), increment t by Δt , and use (2.2) to obtain the predicted solution $\mathbf{x}'_n(t_0) :=$

$\mathbf{x}_n(t_0 + \Delta t)$. We continue this incremental process till the endpoint t_e is reached. We denote $\dot{\mathbf{x}}_n(t)\Delta t$ by $\Delta_n(t)$ and the prediction is obtained by $\mathbf{x}_n(t + \Delta t) = \mathbf{x}_n(t) + \Delta_n(t)$. This sequential process, at the final stage, predicts the optimal solution of interest $\mathbf{x}_n(t_e)$ related to the problem $P_0(t_e)$.

However, after a number of prediction iterations, the predicted solution may deviate from the optimal solution due to numerical imprecision and errors due to approximating integration with a non-infinitesimal step. Hence, the predicted solution $\mathbf{x}'_n(t)$ needs to be corrected [24, 38] by searching for the corrector step $\Delta'_n(t)$ such that:

$$C_0(t): \quad \min_{\{\Delta'_n\}_{n=1}^N} \sum_{n=1}^N a_n(t) f_n(\mathbf{x}'_n + \Delta'_n)$$

$$s.t. \quad \sum_{n=1}^N \mathbf{A}_n \Delta'_n = \mathbf{0}.$$

Using a second-order expansion, the corrector step of $C_0(t)$ can be obtained as:

$$\Delta'_n(t) = \nabla^2 f_n(\mathbf{x}'_n)^{-1} (\mathbf{A}_n^\top \mathbf{d}_2 - a_n(t) \nabla f_n(\mathbf{x}'_n)), \quad n = 1, \dots, N,$$

where

$$\mathbf{d}_2 = \left(\sum_{n=1}^N \nabla^2 f_n(\mathbf{x}'_n)^{-1} \mathbf{A}_n^\top \right)^{-1} \sum_{n=1}^N a_n(t) \nabla^2 f_n(\mathbf{x}'_n)^{-1} \nabla f_n(\mathbf{x}'_n).$$

Some remarks, about the prediction-correction method, are worth pointing out. In practice, the corrected solution is obtained as

$$\text{Corrector Step:} \quad \mathbf{x}''_n(t) = \mathbf{x}'_n(t) + \mu_c \Delta'_n(t), \quad (2.3)$$

where $\mu_c \in (0, 1]$. Furthermore, at each step, the solution is updated, using the corrected solutions, only if $\sum_{n=1}^N a_n(t) f_n(\mathbf{x}''_n) < \sum_{n=1}^N a_n(t) f_n(\mathbf{x}'_n)$.

2.3 Markov Decision Process, Reinforcement Learning, and A2C Algorithm

A Markov Decision Process (MDP) is expressed as a tuple $(\mathcal{S}, \mathcal{A}, P_{\mathcal{G}}(\cdot), r(\cdot))$, where \mathcal{S} is a set of states or the state space, \mathcal{A} is a set of actions or the action space, $P_{\mathcal{G}}(\cdot): \mathcal{S} \times \mathcal{A} \times \mathcal{S} \rightarrow [0, 1]$ is the transition probability describing the system environment, and $r(\cdot): \mathcal{S} \times \mathcal{A} \rightarrow \mathbb{R}$ is the immediate reward function [64]. The system state at time t is denoted by $s_t \in \mathcal{S}$ and the system action at time t is showed by $a_t \in \mathcal{A}$. The transition probability $P_{\mathcal{G}}(s_{t+1}|s_t, a_t)$ shows the probability that being in state s_t and performing action a_t leads to the next state s_{t+1} . Therefore, we have: $s_{t+1} \sim P_{\mathcal{G}}(\cdot|s_t, a_t)$.

The reward function $r(s_t, a_t)$ indicates the immediate reward being obtained by transitioning from state s_t to state s_{t+1} by acting a_t . The action and state spaces can contain continuous-valued or discrete-valued variables or can be finite or infinite.

A policy function $\pi(\cdot)$ is defined to be a mapping function from the state space to the action space. The policy can be deterministic such that the action is determined directly from the state as $a_t = \pi(s_t)$, or it can be stochastic such that the action is randomly drawn from the policy distribution as $a_t \sim \pi(\cdot|s_t)$. Based on the definition of the MDP and Markov property, the probability of trajectory $\tau_T : s_1 \rightarrow a_1 \rightarrow s_2 \rightarrow a_2 \rightarrow \dots \rightarrow s_T$ is determined as:

$$\Pr(\tau_T) := \Pr(s_t, a_t, s_{t+1}, \dots, s_T) = \Pr(s_1) \prod_{t'=t}^T \pi(a_{t'}|s_{t'}) P_{\mathcal{T}}(s_{t'+1}|a_{t'}, s_{t'}).$$

In MDP problems, a cumulative discounted reward $R(t)$ is defined as the summation over an infinite or a finite horizon (T) as:

$$R(t) := \mathbb{E} \left\{ \sum_{t'=t}^T \gamma^{t'-t} r(s_{t'}, a_{t'}) \right\},$$

where $\gamma : 0 < \gamma \leq 1$ is the discount factor. The aim is to find a time-invariant state-dependent policy (deterministic or stochastic), such that the cumulative discounted reward $R(t)$ is maximized:

$$P_1 : \quad \max_{\pi(\cdot)} R(t)$$

$$\text{s.t.} \quad \begin{cases} a_t \sim \pi(\cdot|s_t), \\ s_{t+1} \sim P_{\mathcal{T}}(\cdot|s_t, a_t). \end{cases}$$

When the transition probability is known, P_1 can be viewed as a dynamic optimization problem. For the transition probability being unknown, the problem can be solved by reinforcement learning algorithms. In the context of reinforcement learning algorithms, the notions of exploration and exploitation should be understood. They are two activities by which the algorithm tries to adapt its parameters to the environment to follow an optimal policy. The exploration is the activity by which the algorithm tunes the parameters in the pursuit of what they should optimally be and the exploitation is the activity during which the algorithm uses the already adjusted parameters.

In this thesis, we are interested in a stochastic RL policy, which can properly balance between exploration and exploitation [64], and we assume that state and action space takes continuous values. As such, we focus on the Advantageous Actor-Critic algorithm (A2C) [32, 37], which applies Neural Networks (NNs) for a continuous-valued environment with a stochastic policy. Note that, the NN is used as a policy approximation to circumvent the "curse of dimensionality" issue [13]. In this case, the

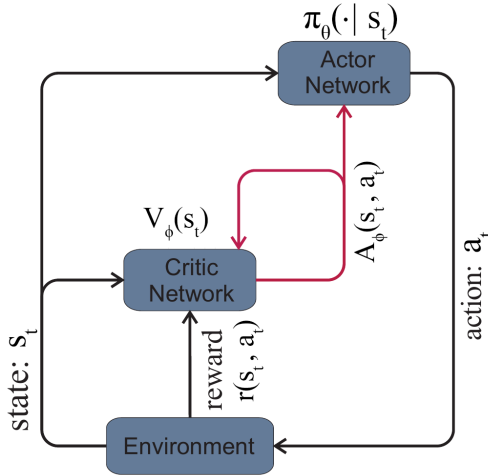


Figure 2.1. The diagram of A2C algorithm. The red arrows show the update processes of actor and critic networks.

policy distribution is expressed by a NN, called the actor network, which is parameterized by a vector θ . The policy is denoted by $\pi_\theta(\cdot|s_t)$. Further, a value-function is defined as the accumulative reward conditioned on starting from a given state s_t :

$$V(s_t) := \mathbb{E} \left\{ \sum_{t'=t}^T \gamma^{t'-t} R(s_{t'}, a_{t'}) \mid s_t \right\}. \quad (2.4)$$

The value function is expressed by another NN, called the critic network, which is parameterized by vector ϕ , so the value-function is denoted by $V_\phi(\cdot)$.

An episodic trajectory is produced by the actor network as follows. For the current state s_t , the actor network produces an action a_t based on the parameter θ . By interacting with the environment based on the transition probability $P_{\mathcal{G}}(\cdot|s_t, a_t)$, an immediate reward $r(s_t, a_t)$ and the next state are generated. The critic network then gives an estimate of the value-function based on s_{t+1} and the parameter ϕ . The produced action, the immediate reward and the value-function are stacked in a buffer to be used in the future to update the parameters of actor and critic networks. By repeating this procedure, the information is buffered until time-slot T . The parameters of the actor and critic networks (θ and ϕ) are updated as follows

$$\begin{aligned} \phi &\leftarrow \phi + \delta \left[\sum_t^T A_\phi(s_t, a_t) \nabla_\phi V_\phi(s_t) \right], \\ \theta &\leftarrow \theta + \psi \left[\sum_t^T A_\phi(s_t, a_t) \nabla_\theta \log(\pi_\theta(a_t|s_t)) + \beta_e \underbrace{\sum_t^T \nabla_\theta H(\pi_\theta(a_t|s_t))}_{\text{Entropy term}} \right], \end{aligned} \quad (2.5)$$

where the advantage value is given by $A_\phi(s_t, a_t) = r(s_{t+1}, a_{t+1}) + V_\phi(s_{t+1}) - V_\phi(s_t)$. The term with the entropy function $H(\cdot)$ is considered in order to trade off exploration against exploitation by discouraging premature convergence to sub-optimal deterministic policies [69]. The parameters ψ and δ are the learning rates corresponding to the update process of actor and critic networks, respectively, and β_e is the entropy regularization term. Figure 2.1 illustrates the A2C algorithm. As Figure 2.1 and (2.5) imply, the parameters of both the actor and critic network are updated using the advantage value generated by the critic network.

3. Cache Models and Methods

In this chapter, the notion of cache policy in cellular networks is first described. Then, the system model utilized throughout this thesis is explained in Section 3.2. We then discuss the cache placement and cache delivery applied for the analysis in Sections 3.3 and 3.4. In Section 3.5, we finally explain the signal propagation model leveraged in this dissertation.

3.1 Cache Policy in Cellular Networks

The data traffic in cellular networks has been explosively increasing [1, 10] causing data congestion and latency when downloading content. Edge caching can be applied to reduce backhaul link congestion and to reduce latency in cellular networks [10, 50]. A cache policy constitutes two successive phases, cache placement and cache delivery. During the cache placement, the popular files are cached at the edge of the network and during the cache delivery the cached files are transmitted towards requesting users. To properly design a cache policy, both of these phases should be considered.

To model the content placement at the caches of BSs, a deterministic [20, 53, 63, 80] or probabilistic [14, 30, 59, 70, 71] approach can be applied. In the probabilistic approach, the contents are cached at the edges of cellular systems based on a common network-wide probability distribution, while in the deterministic method, files are cached based on edge-specific deterministic variables. Deterministic content placement is exploited in [53, 63, 80] to design an optimal cache policy. As such, they formulated the cache policy problem in the edge level with user/BS-related deterministic variables. The notion of probabilistic cache placement has been proposed in [14, 30]. For this, cache-equipped BSs independently and randomly store content at their caches according to a continuous probability distribution. This probability distribution is thus optimized in the network level. Then, cache placement can be implemented over BSs using a decentralised approach. The idea of probabilistic cache placement has

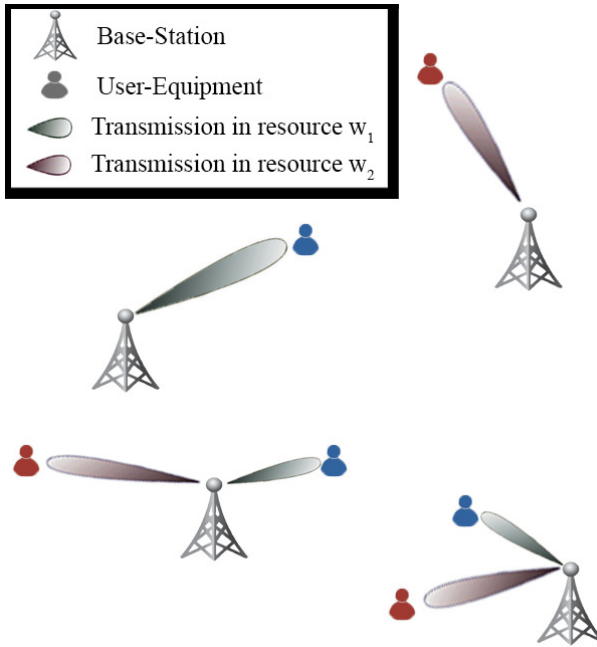


Figure 3.1. Example of a user-centric SPUC networking

been extended to 2-tier cellular networks in [59, 60, 70]. For cache-enabled (Heterogeneous Networks) HetNets with different types of BSs, being differentiated by cache capacity and deployment intensity, the notion of tier-level probabilistic cache placement was discussed in [40, 71]. This placement approach enabled designing a cache policy with network-wide continuous variables using stochastic geometry.

As anticipated in Section 1.1, we focus on probabilistic cache placement in this dissertation, as it can be implemented using a decentralized approach, the cache policy design can be formulated based on continuous optimization variables and the analysis is scalable to large cellular networks due to possibility of using stochastic geometry.

In the cache delivery phase, it is important to distinguish between unicast and multicast approaches, as well as between approaches where a single point (the closest caching BS) delivers a file, and multipoint approaches, where a user downloading a file simultaneously receives transmissions from multiple BSs.

Single-point unicast (SPUC) is an on-demand content delivery scheme for which the cellular network connect each requesting UE to a serving BS to be individually served. Figure 3.1 shows the structure of an SPUC network, for which each requesting UE is served by a BS and there is a single transmission from a BS in a given time-frequency resource. When designing cache policies for SPUC cellular networks, various system assumptions, performance metrics, analytical methods and optimization

approaches have been considered [18, 21, 28, 40, 59, 67, 70, 71, 73, 78].

In [18], a cache-enabled SPUC network is employed where the requesting UEs are responded by the nearest BS. To mitigate the interference level in the network, they use a dynamic network architecture for the considered SPUC such that each BS is active only when a UE demands a content from it. This is in contrast to the conventional SPUC network where the BSs are assumed to be always active. They model the deployment of users and BSs by PPPs, and analyze the system performance in the network level using stochastic geometry. For this, they consider the successful download probability as a metric based on which a cache policy design is formulated.

In [40], a cache-enabled SPUC heterogeneous network with N -tier of BSs is investigated. They applied a multi-tier network to investigate whether it can improve the cache policy compared to a single-tier network. The BSs of different tiers have distinct transmit power, deployment intensity, and cache capacity. In the considered multi-tier SPUC, each UE is associated with the tier that has BS with maximum received power. A tier-specific probabilistic cache placement is applied, where tier k caches file m with probability p_{km} . The deployment of users and BSs are modelled by PPPs. Consequently, they were able to analyze a network metric in the network level using stochastic geometry. For this, the probability of successful delivery is considered as a metric when optimizing the cache policy. They realized that probability of successful delivery of HetNets depends on the cache capacity as well as BS intensities, in contrast to the single-tier networks where it only depends on the cache capacity.

In [70], 2-tier SPUC networking is employed, where macro BSs are connected to the core network and cache-enabled helper nodes are considered. They consider a hybrid cache placement strategy where helper-nodes cache based on a probabilistic strategy while the macro BSs do not cache but fetch the un-cached files on-demand. They model the HetNets using stochastic geometry, and analyze the successful offloading probability, on the network level. This metric is defined as the probability that a requesting user can be responded by a helper node with the data rate greater than a threshold. Usage of stochastic geometry has enabled them to derive a closed-form expression for the global optimal cache policy.

In [67], a cache-enabled multi-tier SPUC network is considered. A tier-specific probabilistic approach is applied for cache placement; file m is cached at tier k with probability p_{km} . They evaluate the optimal cache policy for single-tier and multi-tier networks with respect to the file popularity as well as some tier-specific parameters. The latter parameters include uniform received SIR thresholds, BS transmit powers, BS intensities and cache capacities. They use the cache hit probability as a system metric and exploit stochastic geometry. Using stochastic geometry allowed them to approximate a closed-form expression for the optimal cache placement in the single-tier and multi-tier networks and analyze the impact of received

SIR thresholds and tier-level cache capacities on the optimal cache hit probability.

One of the main disadvantages of SPUC is the severity of interference during downloading a file by a user from its associated BS. It is due to the user-centric base-station association approach that SPUC exploits. In [71], they apply a novel interference management approach for multi-tier SPUC content delivery. More specifically, a two mode tier-level bandwidth allocation is considered with (i) an underlay mode, where each BS randomly selects a subband of the total bandwidth, (ii) an overlay mode where the total bandwidth is divided among tiers of the network, and each BS randomly selects a subband of the bandwidth dedicated to its tier. The probability of successful offloading is optimized with respect to cache placement, bandwidth allocation and a tier-specific frequency reuse factor. Applying network level performance analysis using stochastic geometry, they showed that the overlay mode achieves higher successful offloading probability than the underlay mode.

To mitigate co-channel interference, a multi-antenna beamforming SPUC network is applied in [73], where each user chooses its serving BS or BSs from its K nearest BSs. Considering a probabilistic cache placement, using stochastic geometry and assuming that network is in a high SNR region, enabled them to obtain expressions for the successful transmission probability. The cache placement is then optimized by maximizing a bound of this metric.

Figure 3.2 illustrates a single-point multicast (SPMC) network for which each BS might multicast contents toward multiple UEs, but each UE is served only by one BS. Different structures of SPMC networks and cache policy formulations have been considered in [20, 22, 44, 53, 65, 66, 75]. In these papers, each caching BS multicasts or broadcasts different files towards requesting UEs using a multiple access technique.

A multi-antenna SPMC with deterministic cache placement is considered in [65] to design a cache policy for cache-enabled cloud Radio Access Network (RAN). To cope with the interference problem of SPMC networks by an efficient approach, they apply a sparse multicast beamforming over the BSs. It is noteworthy that they reduce the redundant information flow of SPMC networks, by developing a content-centric network using dynamic file-specific BS clustering. They then formulate a network performance metric based on a weighted sum of the total transmission power and backhaul costs. With deterministic content placement, they have to analyze this metric using edge-specific variables. This metric is thus minimized with respect to cluster-based assignment and beamforming parameters of the BSs.

The idea of tier-specific cache placement is applied for a SPMC HetNet in [22, 66, 75]. To benefit from a diverse content placement, a hybrid cache placement is also included in [22] where an identical placement is

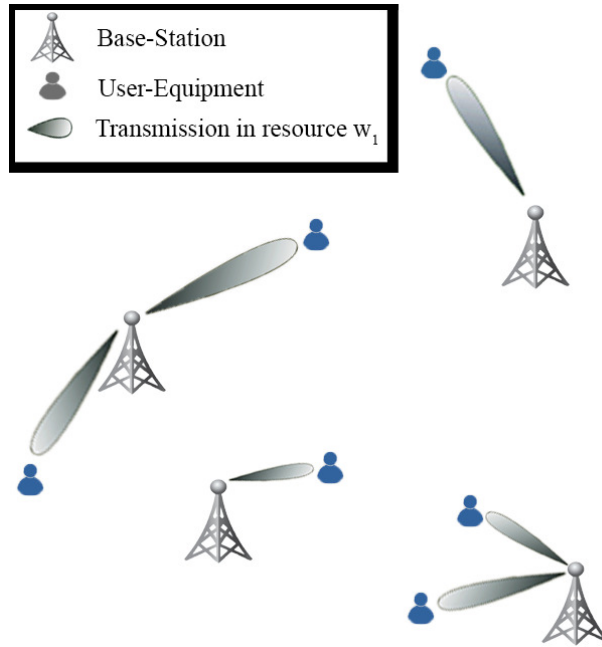


Figure 3.2. Example of an SPMC networking

considered for a macro-tier and a probabilistic one is assumed for a small-cell tier. To mitigate co-channel interference, as a dominating problem of SPMC networks, an interference management approach using resource allocation is used in these papers. More specifically, each BS multicasts k files in the pre-assigned resources each spanning $1/k$ of total bandwidth. The successful transmission probability is then analyzed as a system performance metric. Thanks to stochastic geometry, they managed to find expressions for this metric and find the optimal tier-specific cache placement.

The SPMC approaches discussed above apply a reactive delivery scheme where a file is transmitted only if it is requested by a typical UE. In [44], a proactive SPMC is compared with reactive one for a cache-enabled two-tier network, with one BS and some cache-enabled nodes. For proactive delivery, the files are placed at the caching nodes by BS regardless of receiving file requests. Reactive SPMC can remarkably decrease the resource consumption at the BSs while the proactive method improves the performance at the cost of an increase in the resource consumption.

To alleviate the frequent information passage of conventional SPMC networks, a content-centric single-point multicasting is developed in [53]. As such, a cluster of BSs coordinates to multicast files towards UEs that are grouped based on their content request. In addition, a multicast sparse beamforming is utilized to efficiently mitigate the problem of co-channel interference of SPMC networks. Network power consumption is then

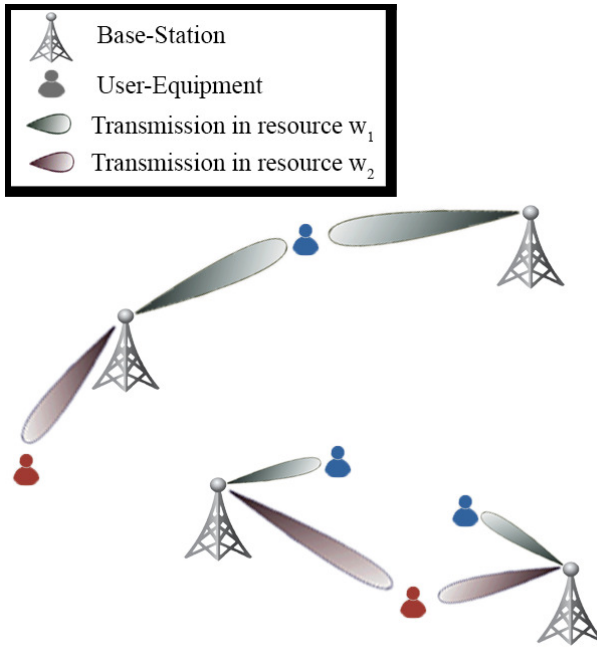


Figure 3.3. Example of an MPUC networking

minimized with respect to a deterministic cache placement and multicast beamforming parameters.

Designing a hybrid transmission scheme to benefit from both unicast and multicast content delivery is studied in [79] for a cellular network with multi-antenna BSs. The authors exploit joint SPUC and SPMC beamforming where beamforming vectors are optimized to maximize the minimum reliable reception rate of the UEs under a BS power constraint. As a deterministic cache placement is leveraged, a hybrid delivery policy is designed based on edge-specific variables.

Figure 3.3 shows a multi-point unicast (MPUC) network for which each UE can be served by multiple BSs but no multiple transmissions happen from a BS in the same time-frequency resource. Deterministic MPUC schemes are considered in [63,80] for on-demand cache delivery. To manage the interference of MPUC networks, a user-specific resource allocation is utilized in [63], where the network-wide resources are orthogonalized between UEs. In such user-centric MPUC networking, each UE receives its requested file based on signals aggregated in the air from multiple caching BSs. A cache policy is thus designed based on edge-specific variables including BS-specific cache placement and user-specific resource allocation vectors.

Information-centric networking can considerably mitigate the redundant information flow across the cellular network as compared to a user-centric method. An information-centric MPUC network is established in [80] using

a Coordinated Multipoint (CoMP) transmission scheme. The information-centricity of this work comes from the fact that all popular files are cached at BSs and coordinately transmitted by all BSs towards users. Managing the interference, a cache-aided zero-forcing beamforming is applied on the BSs. As such, the CSI between UEs and a set of UE-serving BSs is assumed known. However, this scheme still suffers from an unavoidable multiple access interference, as for each UE, unicast CoMP transmissions from the serving set of BSs are applied. As a network performance metric, the average outage probability is minimized with respect to edge-specific variables in order to find an optimal cache placement.

Wireless content delivery based on multipoint broadcast transmissions are applied in Digital Terrestrial TV Broadcasting systems [58]. The LTE system also applies multipoint multicast (MPMC) delivery in the context of enhanced-MBMS [47, 68]. As such, all serving BSs broadcast the same file in a multi-cell transmission mode with an Single-Frequency-Network (SFN) configuration. Hence, the file is concurrently transmitted over the same frequency bandwidth across the whole network. A non-SFN MPMC scheme has been considered together with coded caching at the user end in [12]. In this approach, each transmitter transmits different Minimum Distance Separable (MDS) coded content fragments, and each UE separately decodes transmissions from multiple edge nodes. In this scheme, the only collaboration between BSs comes from the MDS coding, and the BSs are not equipped with caches. Considering that MPMC applies a location-independent broadcasting scheme to transmit contents across the whole network, it can be considered as an Information-Centric Network (ICN). Figure 3.4 portrays an MPMC network for which each UE can be served by multiple BSs and each BS might multicast contents toward multiple UEs in the same time-frequency resource.

From connectivity perspective, it is of benefit to stress the difference among MPMC ICN, user-centric SPUC and connection-centric SPMC networks. In a user-centric network, each requesting UE is connected to a serving BS to receive the needed file, while in a connection-centric network, each file request is associated with a serving BS. In contrast, for MPMC, as an information-centric network, users are proactively satisfied with a network-wide content-specific broadcasting delivery empowered by an in-network caching strategy. For a cellular network with UEs requesting popular files, usage of the information-centric MPMC can remarkably alleviate the backhaul load, though at the price of equipping BSs with caches, compared to the user-centric networks that need considerable redundant transmissions from the core-network using backhaul links.

Having explained different content delivery schemes, it is important to mention that we mainly focus on the information-centric OMPMC (Multipoint Multicast transmission with network-wide file-specific Orthogonal resources) in this dissertation. As declared in Section 1.1, the reason is

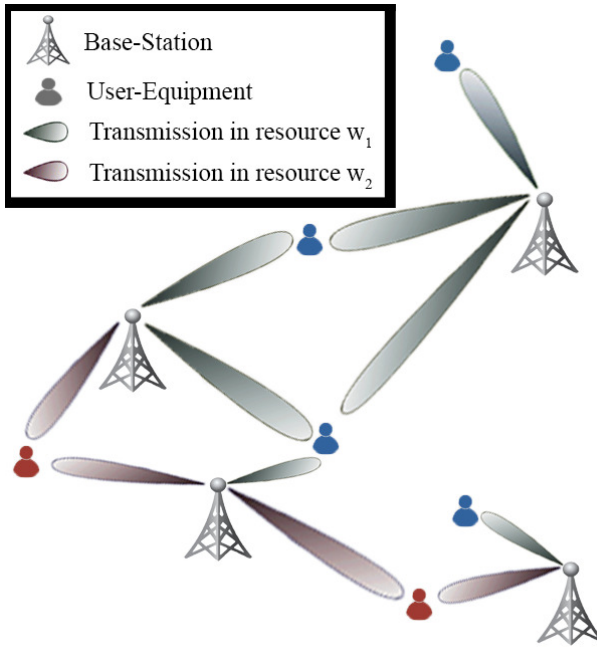


Figure 3.4. Example of an information-centric MPMC networking

that this scheme can outperform other content delivery schemes in networks with considerable numbers of UEs interested in popular contents, as it does not suffer from co-channel interference in transmissions of popular content.

In addition to caching at BSs, caching can be performed at UEs. For this, coded caching can be used as a cache placement approach. Coded caching was originally introduced for a network with a broadcasting server connected to K cache-equipped UEs [45, 46]. Coded caching constitutes two distinct phases, a prefetching phase, and a multicast phase. During the prefetching phase, UEs store segments of files in their limited-capacity caches, and during the multicast phase, the network broadcasts coded messages based on the requested files such that the UEs can retrieve their requested files combining the coded multicast messages with content from their own caches. In [49], the authors showed that the expected transmission load can be considerably decreased when coded caching is applied for files with different popularity, compared to the uncoded caching approaches. In [79], a hybrid delivery scheme based on multicast and unicast beamforming is proposed to cope with the problem that a requested file cannot be completely decoded based on the information of the multicast message and the UE cache.

Coded caching at the multi-antenna user end with MPMC delivery has been considered in [12]. In this approach, each transmitter transmits different Minimum Distance Separable (MDS) coded content fragments, and

each cache-equipped UE separately decodes transmissions from multiple Edge Nodes (EN) using a beamforming multiple access technique.

3.2 System Model

This section introduces the network model exploited in this thesis. We consider a cellular network operating in a time-slotted fashion. In each time-slot, the network tries to satisfy the requests of UEs by applying a content delivery scheme. The network is populated with cache-equipped BSs and UEs. Throughout this thesis, we exploit stochastic geometry to model the deployment of BSs and UEs. As such, BSs and UEs are located according to two independent and homogeneous PPPs.

A content library containing N files is considered from which the BSs proactively store the files at their caches. We assume that files have different popularity, which determines the probability that a distinct file is requested by a randomly selected UE. We assume that the popularity of files is known, unless specified otherwise. Although the methodology applied in this thesis is not restricted to any specific popularity distribution, we consider the Zipf distribution [16, 29] for simulations. Accordingly, f_n denotes the probability that file n is requested, and for the Zipf distribution we have: $f_n = n^{-\tau} / \sum_{j=1}^N j^{-\tau}$ for $n = 1, \dots, N$, where τ denotes the skewness of the Zipf distribution. Notice that the methodology of this thesis is not restricted to any specific popularity model, but we use the Zipf distribution as a conventional model. In this thesis, without loss of generality, we assume that all files have the same size, normalized to one bit.

3.3 Content Placement

In this thesis, probabilistic approach is applied due to its scalability and applicability for large networks. As such, the BSs are equipped with caches of limited storage capacity such that they can store at most M files. BSs independently and randomly cache the files according to a common probabilistic approach as proposed in [14, 59]. More specifically, to store file n , BSs refer to the caching weight $\{q_n\}_{n=1}^N$, $q_n \leq 1$, where q_n indicates the probability that file n is stored at a randomly selected BS. To comply with the capacity of BSs, we have $\sum_{n=1}^N q_n \leq M$.

3.4 Content Delivery and Multipoint Multicast Scheme

As declared, the network operates in a time-slotted fashion. For each time-slot, a spatial distribution of UEs exists, and the UEs request content

according to the popularity of files. In this thesis, the single-point/multi-point unicast transmissions (SPUC/MPUC) and Orthogonal Multipoint Multicast (OMPMC) transmissions are considered as content delivery schemes.

In the following, we explain the mechanisms of the OMPMC cache delivery as one of the main contributions of this research. For a distinct file request, all BSs caching the file simultaneously broadcast it in a resource dedicated to that file. An orthogonal network-wide resource allocation for the files is used. For this, no transmissions occur in the radio resource reserved for a distinct file across the whole network, except the multipoint multicast transmission of this file. The fraction of resources allocated for file n is denoted by w_n , where $\sum_{n=1}^N w_n = 1$.

For the OMPMC scheme, we further assume that the average transmission power of all BSs is the same, denoted by p_{tx} . Moreover, each BS allocates a fractional power $p_{\text{tx}}w_n$ to broadcast file n in dedicated resource w_n . In this case, the transmission Signal-to-Noise-Ratio (Tx-SNR) related to file n is computed as

$$\gamma_n^{(\text{tx})} = \frac{w_n p_{\text{tx}}}{w_n W N_0} = \frac{p_{\text{tx}}}{W N_0} := \gamma_{\text{tx}}, \quad (3.1)$$

where N_0 and W are the noise spectral density and total transmission bandwidth, respectively. As (3.1) suggests, TX-SNR does not depend on file index n .

For OMPMC delivery, wide-band macro-diversity transmission/reception is assumed. Each UE demanding a distinct file receives the corresponding signal over a multipath channel, which is the aggregation of transmitted signals from all BSs caching the file. For this, OFDM SFN transmissions, leveraged in Digital Video Broadcasting [58] can be considered.

3.5 Signal Propagation and System Performance

Here, we describe the model used for the signal propagation as well as the SINR performance of a typical UE being served by the OMPMC delivery scheme.

Based on the MPMC scheme, any file request is fulfilled by all BSs caching that file. Further, the network level resource orthogonality over transmission of different files is used to remove the file-specific interference. We use OFDM-based transmission to deliver files in each dedicated resource. The OFDM receiver performance in the presence of multiple transmitters is analysed in [62]. The dominant multipath feature in the system arises from the multipoint transmissions. In this thesis, we model the signal between an individual BS and a UE in terms of a single-path

channel. Accordingly, the SINR $\gamma_{n,k}$ for UE k requesting file n is:

$$\gamma_{n,k} = \frac{\sum_{j \in \Phi_n} g_{j,k} \|\mathbf{x}_j - \mathbf{r}_k\|_2^{-\beta} b^2(\|\mathbf{x}_j - \mathbf{r}_k\|_2)}{1/\gamma_{\text{tx}} + \sum_{j \in \Phi_n} g_{j,k} \|\mathbf{x}_j - \mathbf{r}_k\|_2^{-\beta} (1 - b^2(\|\mathbf{x}_j - \mathbf{r}_k\|_2))}, \quad (3.2)$$

where $g_{j,k}$ is the shadow fading coefficient between BS j and UE k , \mathbf{x}_j and \mathbf{r}_k are the locations of BS j and UE k , respectively, Φ_n is the set of BSs caching file n . A standard distance-dependent path-loss model is used in (3.2) with a path-loss exponent $\beta > 2$. Further, we assume an Rayleigh distribution for the channel coefficient, i.e., $g_{j,k} \sim \exp(1)$. Moreover, $b(x)$ is a *bias function* which determines the extent of Inter-Carrier Interferences (ICI) and Inter-Block Interference (IBI). As these happen in the same frequency that the desired signal is transmitted, they give rise to co-channel interference. The function $b(x)$ for $x \geq 0$ is expressed as [11, 56]:

$$b(x) = \begin{cases} 1 & \text{for } 0 \leq \frac{x}{c} < T_{cp}, \\ 1 - \left(\frac{x}{cT_s} - \frac{T_{cp}}{T_s} \right) & \text{for } T_{cp} \leq \frac{x}{c} < T_s + T_{cp} \\ 0 & \text{for } \frac{x}{c} \geq T_s + T_{cp}, \end{cases} \quad (3.3)$$

where T_{cp} is the CP length in seconds, T_s is the OFDM symbol length in seconds and c is the speed of light, and the propagation delay is assumed to be directly proportional to the traveled distance. Here, we need to mention that the BSs of OMPMC schedule to simultaneously broadcast their cached files across the network. Then, taking into account the varying distances between the BSs and a typical UE, the UE receives an aggregated signal with different transmission delays, and as such this leads to a delay spectrum of desired-signal and co-channel interference based on the bias function $b(\cdot)$. However, the aired signals from these BSs towards another UE come with completely different delays. (It is not possible to arrange these signals to come to different UEs with the same timing). Nevertheless, this does not make our model not to be a homogeneous Poisson process. By exploiting the Slivnyak-Mecke theorem, focusing on a typical user located at origin and doing the performance analysis, on one hand, and considering different UEs, doing the performance analysis on all of them and then averaging, on the other hand, both lead to a same result. Therefore, we can focus on a typical UE at the origin to perform the analysis. For this, the base-stations located within the range of the cyclic prefix (CP) length or less exclusively contribute to the desired signal. Base-stations positioned within the range of CP length plus symbol length solely contribute to the interference. Base stations falling within the intermediate range between these distances contribute to both the desired signal and interference, with their respective severity determined by the bias function.

For an infinitely long CP, IBI and ICI can be neglected, leading to $b(x) = 1$.

In this case, the SNR $\gamma_{n,k}$ for UE k requesting file n is simplified to:

$$\gamma_{n,k} = \gamma_{\text{tx}} \sum_{j \in \Phi_n} g_{j,k} \|\mathbf{x}_j - \mathbf{r}_k\|_2^{-\beta}. \quad (3.4)$$

In this thesis, we leverage the outage probability as a system metric to assess the performance of the cache policies. This stands for the probability that a typical UE being served by the network is not able to successfully decode the file it is interested in. In what follows, we explain this metric in detail.

The maximum achievable rate is obtained based on the channel capacity in an Additive-White-Gaussian-Noise (AWGN) channel. This rate is specified by the allocated resources and the SINR (SNR) of the message.

The files are transmitted with a rate R_{th} , which is assumed to be same for all the files. Thus a UE experiences an outage if the maximum rate of reliable reception is less than this rate. Since all files are assumed of the same size, we can define a parameter: $\alpha = R_{\text{th}}/W$. Accordingly, the outage probability for UE k requesting file n is expressed as:

$$\mathcal{O}_{n,k} = \Pr(w_n \log_2(1 + \gamma_{n,k}) \leq \alpha). \quad (3.5)$$

Note that if N files are transmitted, the total spectral efficiency of the transmissions is $N\alpha$. The outage probability $\mathcal{O}_{n,k}$ can thus be formulated using the channel gain threshold η_n , as follows:

$$\mathcal{O}_{n,k} = \Pr\left(\frac{\gamma_{n,k}}{\gamma_{\text{tx}}} \leq \eta_n\right), \quad (3.6)$$

where

$$\eta_n = (2^{\alpha/w_n} - 1)/\gamma_{\text{tx}}. \quad (3.7)$$

The outage probability thus can be interpreted based on the normalized SINR $\gamma_{n,k}/\gamma_{\text{tx}}$, such that if the normalized SINR of UE k , downloading file n is less than the corresponding channel gain threshold η_n , the file request is in outage.

4. Orthogonal Multipoint Multicast Cache Policy

In this chapter, following publications P-I and P-V, the probabilistic content placement and OMPMC delivery scheme, as introduced in Chapters 3.2 and 3.3, is studied for cache-enabled cellular networks. A network-wide orthogonal and OFDM-based transmission with sufficiently large CP length is considered for file delivery, as explained in Chapter 3.5, equation (3.4). As such, there will not be any co-channel interference during the file transmission. In this work, the network is modeled using stochastic geometry by deploying the BSs and UEs based on two independent PPPs. An optimal cache scheme is then analyzed, based on cache placement over BSs and resource allocation of OMPMC service.

The overall outage probability is used as a network performance measure. In Section 4.1, an expression is found for it. The problem of cache policy optimization is then formulated in Section 4.2, based on a constrained optimization problem. Joint optimization over the network-wide resource allocation of OMPMC delivery and content placement of cache placement is performed. We then characterize the optimal solution to this problem and devise an algorithm to find the optimal solution. To reduce the computational complexity, we apply a convex relaxation to find a sub-optimal solution. Accordingly, we find a low-complexity algorithm for the solution. An upper bound of the performance gap between the optimal and sub-optimal solution is given. In Section 4.3, we compare the performance of OMPMC cache policy, with the other cache policies from the literature.

4.1 Overall System Outage Probability

In this chapter, we assume that each receiver is able to completely equalize the data without being affected by Inter-Carrier-Interference (ICI) or Inter-Block-Interference (IBI).

We find an expression for the overall outage probability, when the system is modeled using stochastic geometry. The model discussed in Chapter 3.5 is used. According to Slivnyak-Mecke theorem [8], we can compute the

SNR for a UE located at the origin. For this UE, without loss of generality, we can set $\mathbf{r}_0 = 0$ and $\mathcal{O}_n = \mathcal{O}_{n,0}$. Considering that files are requested based on the file popularity $\{f_n\}_{n=1}^N$, the overall outage probability is:

$$\mathcal{O}_{\text{tot}} = \sum_{n=1}^N f_n \mathcal{O}_n, \quad (4.1)$$

where

$$\mathcal{O}_n = \Pr\left(\sum_{j \in \Phi_n} |h_j|^2 \|\mathbf{x}_j\|_2^{-\beta} \leq \eta_n\right). \quad (4.2)$$

Thus, the outage probability of file n can be perceived as the Cumulative Distribution Function (CDF) of the random variable z at a value η_n .

In a network modeled by PPS, we can compute an analytical expression for the OMPMC overall outage probability. It gives an performance criterion that can be used to design the cache policy and draw numerical results. For OMPMC in a network with users being uniformly distributed in space, BSs being distributed according to a homogeneous PPP with intensity λ , a propagation environment characterized by path-loss exponent β , and file $n = 1, \dots, N$ with popularity f_n having caching weight q_n and bandwidth allocation w_n , the overall outage probability is

$$\mathcal{O}_{\text{tot}} = \frac{2}{\pi} \sum_{n=1}^N f_n \int_0^\infty \left\{ \frac{1}{w} \cos\left(\frac{\pi^2 \lambda q_n}{\beta \cos(\pi/\beta)} \left(\frac{w}{\eta_n}\right)^{2/\beta}\right) \exp\left(-\frac{\pi^2 \lambda q_n}{\beta \sin(\pi/\beta)} \left(\frac{w}{\eta_n}\right)^{2/\beta}\right) \times \sin(w) \right\} dw. \quad (4.3)$$

For more details about the derivation of this result, see Publications P-I and P-V. Based on Proposition (4.3), the overall outage probability depends on a specific combination $q_n \eta_n^{-2/\beta}$ of caching weight and channel gain threshold, and not on both separately.

4.2 Resource and Cache Allocation Problem

Based on the overall outage probability being expressed in (4.3), we formulate a joint constrained optimization problem over resource allocation of OMPMC cache delivery $\{w_n\}_{n=1}^N$ and content probability $\{q_n\}_{n=1}^N$ of cache placement. By defining the set $S_N := \{1, \dots, N\}$, the optimal cache policy for OMPMC scheme is expressed as:

$$P_2: \quad \min_{\{q_n\}_{n=1}^N, \{w_n\}_{n=1}^N} \sum_{n=1}^N f_n \mathcal{O}(w_n, q_n), \quad (4.4)$$

$$\text{s.t.} \quad \begin{cases} \sum_{n=1}^N w_n \leq 1, & \sum_{n=1}^N q_n \leq M, \\ 0 \leq w_n \leq 1, & 0 \leq q_n \leq 1, \quad \text{for } n \in S_N, \end{cases}$$

where

$$\mathcal{O}(w_n, q_n) = \mathcal{O}_n = \frac{2}{\pi} \int_0^\infty \frac{1}{w} \cos \left(\frac{\lambda_\beta q_n}{\cos(\pi/\beta)} \left(\frac{w}{\eta_n} \right)^{2/\beta} \right) \exp \left(-\frac{\lambda_\beta q_n}{\sin(\pi/\beta)} \left(\frac{w}{\eta_n} \right)^{2/\beta} \right) \times \sin(w) dw,$$

and $\lambda_\beta := \frac{\pi^2 \lambda}{\beta}$.

We denote the optimal solution of P_2 by $\{w_n^*\}_{n=1}^N$ and $\{q_n^*\}_{n=1}^N$. Some of its crucial properties are:

- If $q_n = 0$, then $\mathcal{O}(w_n, 0) = 1$ for file n regardless of the value of w_n . Likewise, if $w_n = 0$ then $\mathcal{O}(0, q_n) = 1$ regardless of value of q_n .
- $\mathcal{O}(w_n, q_n)$ is a monotonically decreasing function w.r.t. w_n and q_n .
- Without loss of generality, we can order the files according to their popularity. Based on this and second property, the values $\{q_n^*\}_1^N$ and $\{w_n^*\}_1^N$ are decreasing w.r.t. n .
- Based on first property, there exists a $K \in S_N$ such that $w_n = q_n = 0$ for $n > K$.
- At the optimum solution of $P(\beta)$, we have: $\sum_{n=1}^N w_n^* = 1$ and $\sum_{n=1}^N q_n^* = M$.

For more details about these properties, see Publication P-V.

In the sequel, we concentrate on $\beta = 4$. This path-loss exponent has interest in its own right as it is a typical path-loss exponent for moderate and long distances [31]. In this case, the overall outage probability of (4.3) simplifies to:

$$\mathcal{O}_{\text{tot}} = \sum_{n=1}^N f_n \operatorname{erfc} \left(\frac{\pi^2 \lambda q_n}{4\sqrt{\eta_n}} \right), \quad (4.5)$$

where $\operatorname{erfc}(x)$ is the complementary error function, defined as:

$$\operatorname{erfc}(x) = \frac{2}{\sqrt{\pi}} \int_x^\infty \exp(-t^2) dt.$$

By formulating the Lagrange function for P_2 with $\beta = 4$, applying the aforementioned properties, and then taking the derivative with respect to w_n and q_n , it implies that there exists $K \in S_N$ such that:

$$v_1 = -f_n D_{w_n} \mathcal{O}(w_n, q_n), \quad v_2 = -f_n D_{q_n} \mathcal{O}(w_n, q_n) \quad (4.6)$$

for $n \leq K$, and $w_n = q_n = 0$, for $n > K$, where v_1 and v_2 are the Lagrange multipliers related to the equality constraints. Based on second Property, v_1

and v_2 are positive. Further, according to (4.3), we get: $D_{\eta_n} \mathcal{O}_n = \frac{1}{2} \frac{q_n}{\eta_n} D_{q_n} \mathcal{O}_n$, so we have:

$$D_{w_n} \mathcal{O}_n = \frac{\alpha \log(2)}{2} \frac{q_n 2^{\alpha/w_n}}{w_n^2 (2^{\alpha/w_n} - 1)} D_{q_n} \mathcal{O}_n \quad (4.7)$$

Let $v_0^2 = \frac{v_1}{v_2}$, then we get:

$$q_n = v_0^2 \frac{2w_n^2 (2^{\alpha/w_n} - 1)}{2^{\alpha/w_n} \log(2) \alpha}, \text{ for } n \leq K. \quad (4.8)$$

By defining the function $h_0(w_n) := -D_{q_n} \mathcal{O}(w_n, q_n)$ with q_n being replaced based on (4.8), we obtain:

$$\frac{v_2}{f_n} = \frac{2\tilde{\lambda}}{\sqrt{\pi} \sqrt{2^{\frac{\alpha}{w_n}} - 1}} \exp\left(-\tilde{\lambda}^2 v_0^4 (2^{\frac{\alpha}{w_n}} - 1) \left(\frac{2w_n^2}{2^{\frac{\alpha}{w_n}} \alpha \log(2)}\right)^2\right), \text{ for } n \leq K. \quad (4.9)$$

where $\tilde{\lambda} = \frac{\pi^2 \lambda}{4} \sqrt{\gamma_{\text{tx}}}$.

Equations (4.8) and (4.9) are leveraged to find a globally optimal solution of problem P_2 by an algorithm that is devised as follows. We need to find v_0 , v_2 and the optimal solutions $\{w_n^*\}_{n=1}^{K^*}$ and $\{q_n^*\}_{n=1}^{K^*}$ where K^* represents the optimum value of K , which K is the number of files for which the caches and resources will be allocated. The pseudo-code for finding the optimal solution of problem $P_{(4)}$ is presented in Algorithm 1. Since K^* and v_0 are not known in advance, we need to search for them in the corresponding limited intervals. We also seek for v_2 but limit the search space exploiting the fact that $v_{2,\min}(v_0) \leq v_2 \leq v_{2,\max}(v_0)$. We leverage a root-finding method for (4.9) to find $\{w_n\}_1^K$ such that the constraints $\sum_{n=1}^K w_n = 1$ is satisfied. We then find $\{q_n\}_1^K$ based on the obtained $\{w_n\}_1^K$ and using (4.8) so that $|\sum_{n=1}^K q_n - M|^2$ is minimized. Accordingly, we compute the overall outage probability for different values of sought K . After we finalize the searching over possible values of K , we choose K with the smallest outage probability which gives the optimal solution. For more details about this algorithm, see Publication P-V.

In Algorithm (1), there exists two inner loops to search for the optimum values of v_0 and v_2 . This makes it computationally complex. Therefore, it is important to devise a low-complexity solution for problem P_2 . It is achieved using a convex relaxation, and by considering the variable transformation $\xi_n := 1/(2^{\alpha/w_n} - 1)$. Consequently, the relaxed optimization problem is obtained as:

$$\begin{aligned} \tilde{P}_2 : \quad & \min_{K, \{\xi_n\}_{n=1}^N, \{q_n\}_{n=1}^N} \sum_{n=1}^N f_n \mathcal{O}(\xi_n, q_n), \\ & \text{s.t.} \begin{cases} \sum_{n=1}^N \xi_n = K \alpha, & \sum_{n=1}^N q_n = M, & K \in S_N \\ 0 \leq \xi_n \leq \alpha_2, & 0 \leq q_n \leq 1, & \text{for } n \in S_N. \end{cases} \end{aligned} \quad (4.10)$$

Algorithm 1 The Solution of $P_{(4)}$.

- 1: Inputs: $\tilde{\lambda}, \{f_n\}_1^N, M, \gamma_{\text{ref}}, \alpha$.
 - 2: Outputs: Optimal solutions $K^*, (\{w_n^*\}_1^{K^*}, \{q_n^*\}_1^{K^*})$ and \mathcal{O}^* .
 - 3: **for** $K \in S_N$ **do**
 - 4: **for** $v_0 \in [0, v_{0,\text{max}}]$ **do**
 - 5: **for** $v_2 \in [v_{2,\text{min}}(v_0), v_{2,\text{max}}(v_0)]$ **do**
 - 6: Apply a root-finding method over (4.9) to find $\{w_n\}_1^K$ so that $w_{\text{min}} \leq w_n \leq 1$ and $\sum_{n=1}^K w_n = 1$.
 - 7: **end for**
 - 8: Compute q_n for $n \leq K$, based on (4.8).
 - 9: **end for**
 - 10: Select $\{q_n\}_1^K$ that minimize $|\sum_{n=1}^K q_n - M|^2$.
 - 11: Compute $\mathcal{O} = \sum_{n=K+1}^N f_n + \sum_{n=1}^K f_n \operatorname{erfc}\left(\frac{\tilde{\lambda} q_n}{\sqrt{2^{\alpha/w_n} - 1}}\right)$ based on selected $\{q_n\}_1^K$ and $\{w_n\}_1^K$.
 - 12: **end for**
 - 13: Select K providing the smallest outage probability and its corresponding solution. Nominate the optimal solutions by \mathcal{O}^*, K^* and $(\{w_n^*\}_1^{K^*}, \{q_n^*\}_1^{K^*})$.
-

where, $\mathcal{O}(\xi_n, q_n) = \operatorname{erfc}(\tilde{\lambda} q_n \sqrt{\xi_n})$, and $K_\alpha = K(2^{\alpha K} - 1)^{-1}$ and $\alpha_2 = 1/(2^\alpha - 1)$. If \tilde{K} is the optimal value of K for \tilde{P}_2 , then its global solution is:

$$q_n = \begin{cases} h_1^{-1}\left(\frac{v_2}{2\tilde{\lambda}f_n} \sqrt{\frac{\pi M}{\tilde{K}_\alpha}}\right), & n \leq \tilde{K} \\ 0, & n > \tilde{K} \end{cases}, \quad \xi_n = \frac{\tilde{K}_\alpha}{M} q_n,$$

where $h_1(q_n) = \sqrt{q_n} \exp(-\tilde{\lambda}^2 q_n^3 \tilde{K}_\alpha)$, $\tilde{K}_\alpha = \tilde{K}(2^{\alpha \tilde{K}} - 1)^{-1}$, and v_2 is a Lagrange multiplier that is a solution of

$$\sum_{n=1}^K h_1^{-1}\left(\frac{v_2}{2\tilde{\lambda}f_n} \sqrt{\frac{\pi M}{\tilde{K}_\alpha}}\right) = 1.$$

Accordingly, there exists $K \in S_N$ such that for $n > K : q_n = \xi_n = 0$ and for $n \leq K$ we have:

$$\frac{v_2}{2\tilde{\lambda}f_n} \sqrt{\frac{\pi M}{\tilde{K}_\alpha}} = h_1(q_n). \quad (4.11)$$

Applying Jensen's inequality over the convex function $1/h_1(\cdot)$ and considering that $q_n \leq 1$, a lower-bound and an upper-bound can be found for v_2 implying $v_{2,\text{min}} \leq v_2 \leq v_{2,\text{max}}$. Based on these results, an algorithm is devised to find the optimal solution of \tilde{P}_2 . Algorithm 2 presents its pseudo-code. These algorithm provides an approximate solution of problem P_2 . Considering a limited one-dimensional search for v_2 , this solution has a much smaller computational complexity than Algorithm 1. It enables us to obtain the numerical results related to the optimal cache policies for more realistic scenarios.

Algorithm 2 The Solution of \tilde{P}_2 .

- 1: Inputs: $\tilde{\lambda}, \{f_n\}_1^N, M, \gamma_{\text{ref}}, \alpha$.
 - 2: Outputs: Optimal solutions $\tilde{K}, (\{\tilde{\xi}\}_1^{\tilde{K}}, \{\tilde{q}_n\}_1^{\tilde{K}})$ and $\tilde{\mathcal{O}}$.
 - 3: **for** $K \in [1, K_{\text{max}}]$ **do**
 - 4: Set $K_\alpha = \frac{K}{2^{\alpha K - 1}}$.
 - 5: **for** $v_2 \in [v_{2,\text{min}}, v_{2,\text{max}}]$ **do**
 - 6: Apply a root-finding method for (4.11) to find $\{q_n\}_1^K$ so that $q_{\text{min}} \leq q_n \leq 1$ and $\sum_{n=1}^K q_n = M$.
 - 7: **end for**
 - 8: Set $\xi_n = \frac{K_\alpha}{M} q_n$, for $n \leq K$.
 - 9: Compute $\mathcal{O} = \sum_{n=K+1}^N f_n + \sum_{n=1}^K f_n \text{erfc}(\tilde{\lambda} q_n \sqrt{\xi_n})$ based on the obtained $\{q_n\}_1^K$ and $\{\xi_n\}_1^K$.
 - 10: **end for**
 - 11: Select K giving the smallest outage probability and its corresponding solution. Nominate the optimal solutions by $\tilde{\mathcal{O}}, \tilde{K}$ and $(\{\tilde{\xi}\}_1^{\tilde{K}}, \{\tilde{q}_n\}_1^{\tilde{K}})$.
-

4.3 Simulation Results

To benchmark the benefits of orthogonal multipoint multicast caching, two heuristic algorithms were developed, a *hreshold-based* algorithm, and an *Only Bandwidth-optimized* one. Furthermore, a network-wide resource allocation Single-Point Multicast (SPMC) scheme was considered based on the literature.

4.3.1 Threshold-Based OMPMC Scheme

A simplified *threshold based* policy is developed based on a threshold $v \in S_N$. For files less popular than file v , no resources are allocated, while equal resources will be allocated to the other files. Therefore, if $n > v$, we set $w_n = q_n = 0$, otherwise, we set $w_n = q_n/M = 1/v$. We name the resulting cache policy as OMP – th.

4.3.2 Only Bandwidth-Optimized OMPMC Scheme

A sub-optimal cache policy is considered where only the bandwidth allocation is optimized and the cache placement is based on a simple method. As such, we follow the cache placement strategy: $q_n = Mf_n$, for $n \in S_N$. However, in order to comply with $q_n \leq 1$, we bound any q_n whose value exceeds 1, and increase others such that $\sum_{n=1}^N q_n = M$. We call the resulting cache policy OMP – w.

Table 4.1. Cache Policy Approaches

Policy	Network-Wide Bandwidth Allocation	Cache Allocation	Transmission Scheme
OMP	Yes	Yes	OMPMC
OMP-w	Yes	$p_n \sim f_n$	OMPMC
OMP-th	On-off-threshold	On-off-threshold	OMPMC
OSP	Yes	Yes	SPMC

4.3.3 Single-Point Scheme from the Literature

To have a fair comparison, a SPMC scheme with network-wide resource allocation across files is taken into account. We denote this policy by Orthogonal Single-Point (OSP). For this policy, each BS can simultaneously transmit several files in disjoint radio resources, so M can be greater than one. Based on the analytical expression in [7], the overall outage probability for this cache policy is:

$$\mathcal{O}_{\text{tot}}^{\text{OSP}} = 1 - \sum_{n=1}^N \frac{\sqrt{\pi^3} \lambda f_n q_n}{\sqrt{4\eta_n}} \exp\left(\frac{\kappa_n^2}{\eta_n}\right) \operatorname{erfc}\left(\frac{\kappa_n}{\sqrt{\eta_n}}\right),$$

where $\kappa_n = \frac{\lambda \pi q_n}{2} \left(1 + \sqrt{\eta_n \gamma_{\text{tx}}}\right) \tan^{-1}(\sqrt{\eta_n \gamma_{\text{tx}}})$, with η_n from (3.7).

4.3.4 Performance Results

The evaluated cache policies and their properties are tabulated in Table 4.1.

For the comparison, we consider settings based on [40]. The number of files is set as $N = 200$ and the cache capacity to $M = 20$. Two values for the skewness are considered; $\tau = \{0.8, 2.6\}$ and the spectral efficiency threshold is set to $\alpha = 0.05$. For signal propagation, we apply an Urban NLOS scenario from 3GPP standard [2] with carrier frequency 2 GHz and BS transmission power 23 dBm. The antenna gain at the UE and BS are 0 dBi and 8 dBi, respectively, the noise-figure of UE is 9 dB, the noise spectrum density is -174 dBm and the bandwidth is 20 MHz. We consider the path-loss exponent: $\beta = 4$. These values result in the reference SNR to be $\gamma_{\text{tx}} = 0.105$.

The overall outage probability in this scenario is plotted in Figure 4.1 as a function of cache intensity for skewness $\theta = 2.6$. The OMP policy outperforms other cache strategies for all evaluated cache intensities. Note that, the outage probability of OSP becomes independent of the intensity as cache intensity increases. By increasing cache intensity, the effect of thermal noise is decreasing for OSP policy, and the network becomes interference-limited. The multicast multipoint delivery methods are noise-limited,

and the noise limitation decreases with increasing cache intensity, as the received power grows. As the intensity increases OMP – w diverges from the optimal solution. For most evaluated cache intensities, the OMP – th gives an acceptable result.

For skewness $\theta = 0.8$, the overall outage probability is shown in Figure 4.2. The OMP and OMP – th policies outperform OSP in this scenario as well. As cache intensity increases, the outage probability improves for all policies except OSP, which is limited by co-channel interference. Further, as the cache intensity grows, the solution of OMP – th becomes more reliable compared to the result of OMP – w.

Figure 4.3 shows the resource allocation of cache solution as a function of the file index for cache intensity $\lambda = 30$ and skewness $\tau = 2.6$. For the OSP policy, the resources are allocated only to a few popular files, while for the OMP policy, around 40 percent of files can be accommodated in the total bandwidth. For the latter policy, the allocated resources decrease as specified by property A.2, while for the OMP – w they grow since the caching weights are not optimized.

4.4 Conclusion

In this chapter, we considered cache placement and delivery based on a network-wide OMPMC transmission scheme. A cache policy jointly optimizing cache placement and radio resource allocation was formulated, based on the derived expression of the outage probability. An algorithm was devised to obtain the optimal solution for $\beta = 4$, where the optimization objective can be written in closed form. A low-complexity algorithm was proposed to obtain a sub-optimal solution. The solution was characterized by a file popularity threshold, with files less popular than the threshold, they are neither cached nor delivered. We compared the outage performance of OMPMC based on the devised low-complexity algorithm with single-point multicast from the literature. Simulation results showed that the outage probability of OMPMC outperforms other delivery strategies for different cache intensities, UE intensities and spectral efficiency thresholds. The usage of the OMPMC delivery scheme can be considered as a promising technique to be employed by the cache-enabled networks.

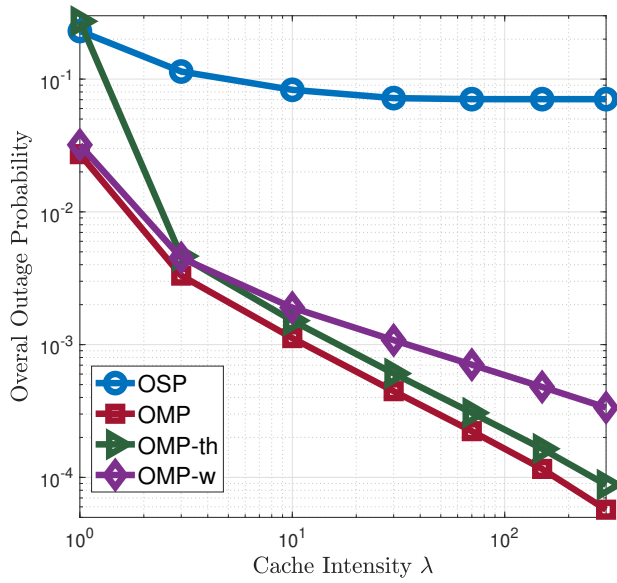


Figure 4.1. The overall outage probability as a function of cache intensity for skewness $\tau = 2.6$, $N = 200$ and $M = 20$.

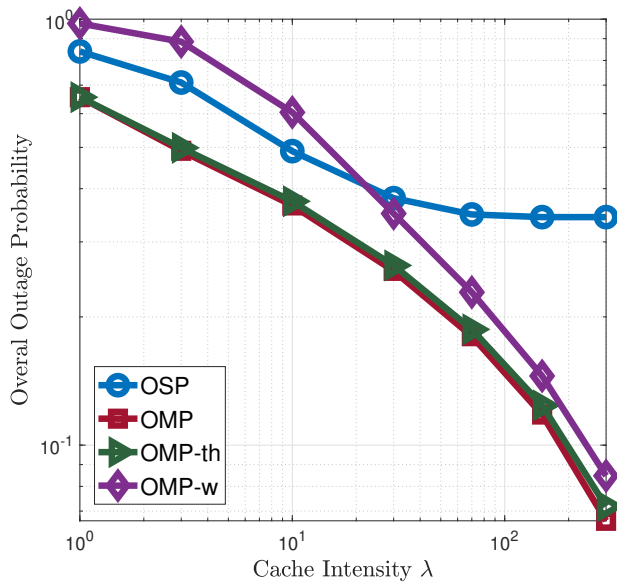


Figure 4.2. The overall outage probability as a function of cache intensity for skewness $\tau = 0.8$, $N = 200$ and $M = 20$.

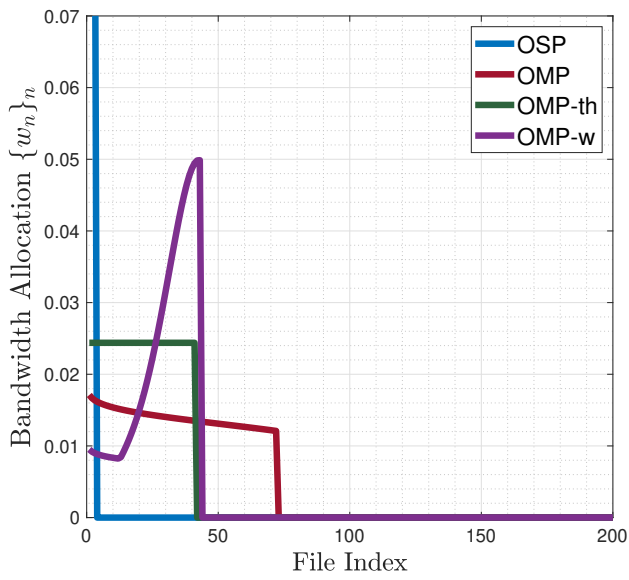


Figure 4.3. The bandwidth allocation as a function of file index for cache intensity $\lambda = 30$ and skewness $\tau = 2.6$.

5. Multipoint Multicast Caching With ICI and IBI

In this chapter, following publications P-II and P-VI, the probabilistic content placement and OMPMC delivery scheme, as introduced in Chapters 3.2 and 3.3, is studied for cache-enabled cellular networks. In contrast to the previous chapter, here we consider the effect of interference arising from the multipoint transmission. A network-wide orthogonal OFDM-based interference-aware transmission is considered for content delivery, as explained in Chapter 3.5 equation (3.2). The simultaneous OMPMC transmissions create artificial multipath propagation, which produces IBI and ICI in OFDM systems. In this work, the network is modeled using stochastic geometry by deploying the BSs and UEs based on two independent PPPs. An optimal cache scheme is then analyzed, based on cache placement over BSs and resource allocation of OMPMC service.

In Section 5.1, an expression is found for the overall outage probability as a network performance. The problem of interference-aware cache policy is then formulated, in Section 5.2, based on a constrained optimization problem jointly over the network-wide resource allocation of OMPMC delivery and content placement of cache placement, with consideration of IBI and ICI. Considering that the outage probability does not have a closed-form expression, we exploit the prediction-correction method, explained in Chapter 2.2, to find the optimal solution. As such, Section 5.3 is devoted to explain a prediction-correction-based cache policy algorithm. In Section 5.4, we benchmark the performance of OMPMC interference-aware cache policy, which reveals some intuitions about the effect of ICI/IBI on cache policy.

5.1 Overall System Outage Probability

We choose the overall outage probability as a network system performance. Stochastic geometry is leveraged to find an expression for this metric. In contrast to Chapter 4, here we develop an interference-aware policy, where IBI and ICI arising from realistic values for the CP length is taken into

account. SINR is computed as explained in (3.2). According to Slivnyak-Mecke theorem [8], we can compute the SINR for a UE located at the origin. For this UE, without loss of generality we can set $\mathbf{r}_0 = 0$ and $\mathcal{O}_n = \mathcal{O}_{n,0}$. Considering that files are requested based on the file popularity $\{f_n\}_{n=1}^N$, the overall outage probability is:

$$\mathcal{O}_{\text{tot}} = \sum_{n=1}^N f_n \mathcal{O}_n, \quad (5.1)$$

where

$$\mathcal{O}_n = \Pr\left(\sum_{j \in \Phi_n} g_j \|\mathbf{x}_j\|_2^{-\beta} k_n(\|\mathbf{x}_j\|_2) \leq \eta_n\right), \quad (5.2)$$

and $k_n(x) = (1 + \gamma_{\text{tx}} \eta_n) b^2(x) - \gamma_{\text{tx}} \eta_n$.

Accordingly, for the OMPMC in a network with BSs distributed according to a homogeneous PPP with intensity λ , with a propagation environment characterized by path-loss exponent β , an OFDM transmission scheme with symbol length T_s and CP length T_{cp} and file $n = 1, \dots, N$ with popularity f_n having caching weight q_n and bandwidth allocation w_n , the overall outage probability is

$$\begin{aligned} \mathcal{O}_{\text{tot}} = & \frac{1}{2} - \frac{1}{\pi} \sum_{n=1}^N f_n \int_0^\infty \frac{1}{w} \sin\left(-w\eta_n + 2\pi\lambda q_n w \int_0^\infty \frac{r^{1-\beta} k_n(r)}{w^2 r^{-2\beta} k_n(r)^2 + 1} dr\right) \\ & \times \exp\left(-2\pi\lambda q_n w^2 \int_0^\infty \frac{r^{1-2\beta} k_n(r)^2}{w^2 r^{-2\beta} k_n(r)^2 + 1} dr\right) dw. \end{aligned} \quad (5.3)$$

For more details about the derivation of this result, see Publication P-II and P-VI.

5.2 Resource and Cache Allocation Problem

Based on the overall outage probability (4.3), we formulate a joint constrained optimization problem over resource allocation of OMPMC cache delivery $\{w_n\}_{n=1}^N$ and content probability $\{q_n\}_{n=1}^N$ of cache placement. By defining the set $S_N := \{1, \dots, N\}$, the optimal cache policy for OMPMC scheme is expressed as:

$$\begin{aligned} P_3 : \quad & \min_{\{q_n\}_{n=1}^N, \{w_n\}_{n=1}^N} \sum_{n=1}^N f_n \mathcal{O}(w_n, q_n), \\ & \text{s.t.} \begin{cases} \sum_{n=1}^N w_n \leq 1, & \sum_{n=1}^N q_n \leq M, \\ 0 \leq w_n \leq 1, & 0 \leq q_n \leq 1, \quad \text{for } n \in S_N, \end{cases} \end{aligned} \quad (5.4)$$

where $\mathcal{O}(w_n, q_n)$ is the outage probability of file n which depends on w_n and q_n . Some of crucial properties of P_3 are:

- If $p_n = 0$, then $\mathcal{O}(w_n, p_n) = 1$ regardless of the value of w_n . Likewise, if $w_n = 0$, then $\mathcal{O}(w_n, p_n) = 1$ regardless of the value of p_n .
- $\mathcal{O}(w_n, p_n)$ is a monotonically decreasing function w.r.t. w_n and p_n .
- Without loss of generality, we can sort the files according to their popularity. Based on this and the second property, the values \mathbf{w} and \mathbf{p} are decreasing w.r.t. n .
- As a consequence of the first property, there exists a $K \in S_N$ such that $w_n = p_n = 0$ for $n > K$.
- Based on the second property, at the optimum solution of P_3 , the cache capacity and total bandwidth constraints are satisfied with equality; $\sum_{n=1}^N p_n = 1$ and $\sum_{n=1}^N w_n = 1$.

Considering that the objective function of problem P_3 lacks a closed form expression, we use an approach in the line with Homotopy Continuation, explained in Chapter 2.2. For that, we formulate a parametric optimization problem exactly as P_3 but with θ -parameterized file popularity $a_n(\theta)$ replacing f_n . We denote this parametric optimization problem with $P_3(\theta)$. For $a_n(\theta)$, we need to have: $\lim_{\theta \rightarrow 0} a_n(\theta) = \frac{1}{N}$ and $\lim_{\theta \rightarrow \tau} a_n(\theta) = f_n$, where τ is the skewness of the popularity distribution. By defining $\mathbf{x}_n = [w_n, q_n]^\top$ and $S_K := \{1, \dots, K\}$, the following ODEs related to P_3 can be derived, based on the aforementioned properties:

$$\frac{d\mathbf{x}_n}{d\theta} = \mathbf{H}_n^{-1}(\mathbf{c} - \dot{a}_n(\theta)\nabla\mathcal{O}_n(w_n, p_n)), \quad n \in S_K, \quad (5.5)$$

where

$$\mathbf{c} = \left(\sum_{n=1}^K \mathbf{H}_n^{-1} \right)^{-1} \sum_{n=1}^K \left(\mathbf{H}_n^{-1} \dot{a}_n(\theta)\nabla\mathcal{O}_n(w_n, p_n) \right), \quad (5.6)$$

and

$$\mathbf{H}_n = a_n(\theta)\nabla^2\mathcal{O}_n(w_n, p_n). \quad (5.7)$$

Here $\nabla\mathcal{O}_n(w_n, p_n)$ and $\nabla^2\mathcal{O}_n(w_n, p_n)$ indicate the Gradient vector and Hessian matrix of $\mathcal{O}_n(w_n, p_n)$ w.r.t. w_n and p_n . For more details, see Publication P-II and P-VI.

The problem $P_3(\theta)$ has a trivial optimal solution for $\theta = 0$, when the popularity is flat, which is $(w_n, q_n) = (\frac{1}{K}, \frac{M}{K})$ for $n \in S_K$. Therefore, by solving the ODEs (5.5) for the initial point $\theta = 0$, $\{w_n\}_n = 1/K$, $\{p_n\}_n = M/K$ and the target point $\theta = \tau$, $\{w_n\}_n, \{p_n\}_n$, the optimal solution of P_3 is obtained, assuming K . Hence, by solving these ODEs, the optimal solution of P_3 can be found assuming existence of \mathbf{H}_n^{-1} and $\left(\sum_{n=1}^K \mathbf{H}_n^{-1} \right)^{-1}$.

Algorithm 3 The prediction-correction algorithm for cache policy.

- 1: **for** $K \in \mathcal{K}$ **do**
 - 2: **Initialization:**
 Set $\theta = 0$ and $(w_n, p_n) = (\frac{1}{K}, \frac{1}{K}), \forall n \in \{1, \dots, K\}$.
 - 3: **while** $\theta' \leq \tau$ **do**
 - 4: Increment the popularity distribution, $\theta' = \theta + \Delta\theta$.
 - 5: **Predictor step:**
 Find $(\Delta w_n, \Delta p_n)$ from (5.5) and (5.6) and obtain
 $w'_n = w_n + \Delta w_n, p'_n = p_n + \Delta p_n$.
 - 6: **Corrector step** (if necessary):
 Find $(\Delta w'_n, \Delta p'_n)$ from (5.8).
 - 7: **if** $\sum_{n=1}^K a_n(\theta') \mathcal{O}_n(w'_n, p'_n) < \sum_{n=1}^K a_n(\theta) \mathcal{O}_n(w'_n, p'_n)$ **then**
 - 8: Update the solution by:
 $w''_n = w'_n + \mu_c \Delta w'_n, p''_n = p'_n + \mu_c \Delta p'_n$.
 - 9: **else**
 - 10: $w''_n = w'_n, p''_n = p'_n$.
 - 11: **end if**
 - 12: Set $\theta = \theta', w_n = w''_n$ and $p_n = p''_n$.
 - 13: **end while**
 - 14: Save $\{p_n\}_{n=1}^K, \{w_n\}_{n=1}^K$ and the overall outage probability related to index K .
 - 15: **end for**
 - 16: Search over K to find the optimum cache policy.
-

5.3 A prediction-correction Algorithm for Optimal Cache policy

We resort to a numerical method to obtain the solution. As such, we leverage the prediction-correction method, explained in Chapter 2.2. For the predictor step, we use (2.2), and for the corrector step, we use (2.3) where:

$$\begin{aligned}
 \Delta'_n &= \mathbf{H}'_n{}^{-1} (\mathbf{c}' - a_n(\theta) \nabla \mathcal{O}_n(w'_n, p'_n)), \quad n \in S_K, \\
 \mathbf{c}' &= \left(\sum_{n=1}^K \mathbf{H}'_n{}^{-1} \right)^{-1} \sum_{n=1}^K \left(\mathbf{H}'_n{}^{-1} a_n(\theta') \nabla \mathcal{O}_n(w'_n, p'_n) \right) \\
 \mathbf{H}'_n &= a_n(\theta) \nabla^2 \mathcal{O}_n(w'_n, p'_n), \tag{5.8}
 \end{aligned}$$

and $\Delta'_n = [\Delta w'_n, \Delta p'_n]^T$. For the popularity parametrization, $\{a_n(\theta)\}_{n=1}^N$ is chosen such that the need for corrector step is minimized, for this we set $a_n(\theta) = \frac{1}{N} (N f_n)^{\theta/\tau}$, for $n \in S_N$.

A pseudo code for the prediction-correction method to find the solution of P_3 is given in Algorithm 3. Note that we perform a one-dimensional search over a candidate set \mathcal{K} to find the optimum value for K .

5.4 Simulation Results

The result of prediction-correction Method for the Interference-Aware policy is indicated by PCM – IA. To benchmark the benefits of this policy, some policy schemes were additionally considered based on the "Threshold-based" and "Interference-Ignoring" solutions. In the followings, we describe these solutions.

5.4.1 Threshold-based Solution

A simplified *threshold based* policy is developed based on a threshold $\nu \in S_N$. For files less popular than file ν , no resources are allocated, while equal resources will be allocated to the other files. Therefore, if $n > \nu$, we set $w_n = q_n = 0$, otherwise, we set $w_n = q_n/M = 1/\nu$. We call the resulting cache policy OMP – th.

5.4.2 Interference-Ignoring Solution

The cache policy of Chapter 3 is directly used despite the presence of ICI/IBI. For this, the overall outage optimization problem (4.4) is solved using the prediction-correction Method. Recall that the obtained solution is evaluated in the presence of ICI/IBI. We denote the obtained solution by PCM – II.

Having specified the "Threshold-based" and "Interference-Ignoring" solutions, we consider the TB – IA policy scheme which is the "Threshold-Based Interference-Aware" solution, and TB – II policy scheme which is the Threshold-Based Interference-Ignoring solution. The policy scheme TB – II is explained in Chapter 4.3 and is applied despite the presence of ICI/IBI.

5.4.3 Performance Results

For the numerical comparison, the number of files is set to $N = 100$ and the value of cache capacity to $M = 10$. Two values for the skewness are considered; $\tau = \{0.6, 2.6\}$, and the spectral threshold is set to $\alpha = 0.1$. For the signal propagation settings, we apply an Urban NLOS scenario from 3GPP standard [2] with carrier frequency 3.5 GHz and the transmission power of BSs 33 dBm. The antenna gain at the UE and BS are 0 dBi and 5 dBi, respectively, the noise-figure of UE is 9 dB, the noise spectrum density is -174 dBm and the bandwidth is 20 MHz. We consider the path-loss exponent: $\beta = 4$. These values lead the reference SNR to be $\gamma_{\text{tx}} = 0.105$.

Figure 5.1 shows the overall outage probability obtained with different caching policies as a function of the CP length for skewness $\tau = 2.6$ and effective intensity $\lambda_{\text{eff}} := M \times \lambda = 3 \times 10^3$. The PCM – IA policy outperforms other policies for all values of CP length. There is a remarkable performance gap

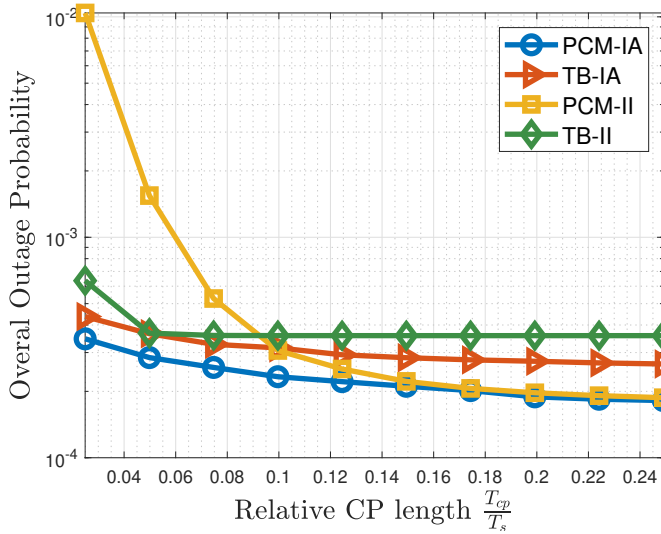


Figure 5.1. The overall outage probability as a function of ratio of CP length to the symbol length for skewness $\tau = 2.6$ and effective intensity $\lambda_{\text{eff}} = 3 \times 10^3$.

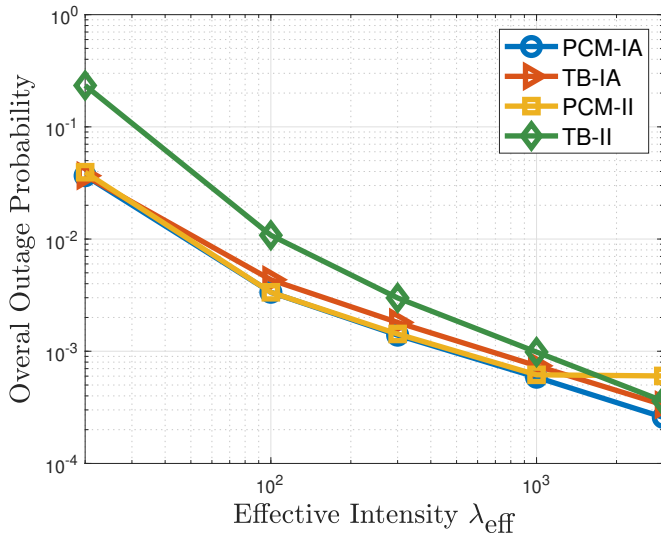


Figure 5.2. The overall outage probability as a function of the effective intensity λ_{eff} for skewness $\tau = 2.6$, and relative CP length 7%.

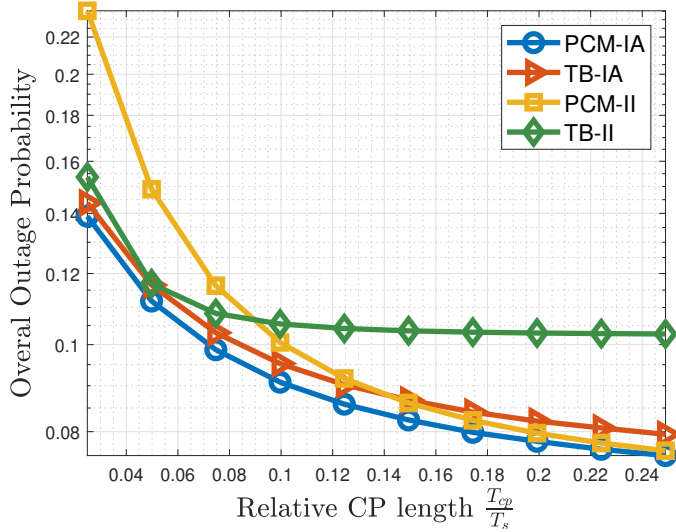


Figure 5.3. The overall outage probability as a function of ratio of CP length to the symbol length for skewness $\tau = 0.6$ and effective intensity $\lambda_{\text{eff}} = 4 \times 10^3$.

between Interference-Ignoring policies especially for short CPs. As the CP length increases, the performance gap between PCM-IA, and TB policies grows. Note that the TB policies develop an error floor despite increasing CP length. Overall, these results portray that the effect of ICI/IBI has to be considered in optimization and show the merit of PCM-IA when designing an optimal cache policy. Interestingly, the TB-II policy is more robust against interference than the PCM-II policy, when CP is short and the interference is accordingly strong.

Figure 5.2 shows the overall outage probability as a function of the effective cache intensity λ_{eff} for skewness $\tau = 2.6$ and normal CP length $T_{\text{cp}} = 4.7 \mu\text{s}$, corresponding to the CP-length ratio 7%. The PCM-IA method outperforms the TB policies. This is expected, since with PCM-IA, resources are optimally allocated, in contrast to equal allocation in the TB policies. For high cache intensities, the Interference-Ignoring solution PCM-II becomes unstable, and exhibits cross-over to an interference limited regime.

Figure 5.3 shows the outage probability results for skewness $\tau = 0.6$ and effective intensity $\lambda_{\text{eff}} = 4 \times 10^3$. As more caching is needed with a smaller skewness, a larger value of effective intensity is used as compared to Figure 5.1. We again find that the Interference-Ignoring solutions are less reliable than Interference-Aware policies. As the CP length increases, the reliability of TB-II considerably decreases and becomes saturated.

Overall, with the considered OFDM parametrizations and network densities, the effect of ICI/IBI has a considerable role for higher caching

intensities λ . This can be understood as follows: If there is no ICI/IBI, the statistics of SINR experienced by UEs improve indefinitely with caching densification. As a consequence, with increasing λ one can reduce the outage of the cached files, or use less resources per file, and cache more files; both methods reduce the overall outage. When there is ICI/IBI, the network becomes interference limited; the statistics of SINR become asymptotically independent of λ . As a consequence, an outage floor develops asymptotically in λ . In the plots, we see these floors starting to have an effect.

5.5 Conclusion

In this chapter, we considered OMPMC caching in OFDM cellular networks. The optimal cache placement policy with ICI and IBI was obtained by formulating a time-varying optimization problem. The outage probability was analyzed based on stochastic geometry analysis. A prediction-correction method was devised to find the optimal cache policy considering ICI and IBI. We found that taking the ICI/IBI into account in cache placement and delivery optimization provides systematically better results than neglecting it.

6. Hybrid Cache-enabled Traffic Offloading with Single-point Unicast

The optimal probabilistic cache policy for the OMPMC network was studied in the previous chapters. In this chapter, following publication P-III, a hybrid delivery scheme, comprising the OMPMC and SPUC components, is considered and an optimal cache policy is accordingly designed. For the hybrid scheme, the traffic is offloaded from the SPUC component using network-wide OMPMC transmission. In order for these two components to cooperate in content delivery, the files are classified into two sets. The most popular files are cached at the BSs using a probabilistic approach and are served by OMPMC, as explained in Chapters 3.3 and 3.5. The remaining files are fetched from the core network on demand and served by SPUC. An optimal hybrid scheme is then analyzed, based on resource allocation between OMPMC and multi-antenna SPUC components.

In Section 6.1, we explain the structure of the hybrid caching scheme. A closed-form expression is derived in Section 6.2 for the total outage probability of the hybrid scheme using stochastic geometry. Section 6.3 is devoted to formulating a constrained optimization problem to design the cache policy. The optimal solution is obtained by finding optimal cache placement, bandwidth allocation, and file classification index. We exploit the prediction-correction method, explained in Chapter 2.2, to find the optimal solution. In Section 6.4, we show the simulation results for the performance of the optimal caching using the hybrid scheme.

6.1 Hybrid Delivery Scheme

In this chapter, we consider the same model for the cellular network and BSs as discussed in Chapters 3.2 and 3.3. However, the cache-implemented BSs are also equipped with L antennas. We establish a hybrid delivery scheme based on a combination of OMPMC and SPUC components over the BSs to fulfill UE requests. These components utilize network-wide disjoint resources for file transmission, W^{MM} for the OMPMC component and W^{SU} for the SPUC one. For the hybrid scheme, we classify the files

into two sets, the popular set \mathcal{F}_1 and the unpopular set \mathcal{F}_2 . The popular set \mathcal{F}_1 is broadcasted by the OMPMC component as discussed in Chapter 3.5, and the unpopular set \mathcal{F}_2 is served by the multi-antenna on-demand SPUC component. The SPUC operates as a conventional cellular network [21, 40, 67, 70, 71, 73]. The requesting UEs are served by their nearest BSs, and the requested file is fetched from the core network and unicast towards the requesting UE.

The overall outage probability of OMPMC service has been investigated in Chapters 4. In the next section, we investigate the outage probability of SPUC service and hybrid scheme.

6.2 Hybrid Outage Probability

We first analyze the SINR of the SPUC scheme. The BSs constitute a Voronoi tessellation with different cells [19]. The size of a Voronoi cell A is based on a gamma distribution that depends on the BSs intensity λ . The BS of each Voronoi cell responds to U UEs, where U follows a Poisson distribution, which depends on the cell size A and the UE intensity λ_{UE} [17, 76]. We apply zero-forcing beamforming in each Voronoi cell to respond to these U UEs. Consequently, the SINR for requesting UE k , in a Voronoi cell, is expressed as:

$$\gamma_k^{\text{SU}} = \frac{g_{0,k} \|\mathbf{x}_0 - \mathbf{r}_k\|_2^{-\beta}}{1/\gamma_{\text{tx}} + \sum_{j \in \Phi/0} g_{j,k} \|\mathbf{x}_j - \mathbf{r}_k\|_2^{-\beta}}, \quad (6.1)$$

where $g_{0,k}$ is the effective channel gain between nearest BS and UE k , constructed from the channel vector and the beamforming vector. The location of the BS nearest to UE k is \mathbf{x}_0 , the set $\Phi/0$ represents all BSs except the nearest BS, and $g_{j,k}$ is the effective channel gain from BS j to UE k . In each cell, if $L \leq U$, all UEs are served by the nearest BS, otherwise, it randomly selects L UEs to respond. Consequently, we have $g_{0,k} \sim \Gamma(\max(L-U+1, 1), 1)$ and $g_{j,k} \sim \Gamma(\min(L, U), 1)$ [19, 34], where $\Gamma(a, b)$ is the gamma distribution with shape a and scale b .

We now analyze the outage probability of the SPUC component. If $L \geq U$ the outage probability for UE k served by SPUC is expressed as:

$$\mathbb{E}_{U,A} \left\{ \Pr(W^{\text{SU}} \log(1 + \gamma_k^{\text{SU}}) \leq 1) \right\}, \quad (6.2)$$

where $\mathbb{E}_X\{\cdot\}$ indicates the expected value with respect to X . However, if $L < U$ some UEs in the cell are in outage. Therefore, a specific UE is served by its nearest BS with the probability $P_U = \min(\frac{L}{U}, 1)$. Overall, the outage probability for this scheme becomes:

$$\mathcal{O}_k^{\text{SU}} = \mathbb{E}_{U,A} \left\{ (1 - P_U) + P_U \Pr(W^{\text{SU}} \log(1 + \gamma_k^{\text{SU}}) \leq 1) \right\}. \quad (6.3)$$

Based on the Slivnyak-Mecke theorem [8], we can analyze the outage probability of SPUC service, for a UE located at the origin. As such, we set $\mathbf{r}_0 = 0$, $g_j = g_{j,0}$, and $\mathcal{O}_0^{\text{SU}} = \mathcal{O}^{\text{SU}}$. For the SPUC scheme applying zero-forcing beamforming with bandwidth W^{SU} serving a set of files \mathcal{F}_2 , with BSs equipped with L antennas and distributed according to a PPP with intensity λ , and UEs distributed according to another PPP with intensity λ_{UE} , in an environment with path-loss exponent $\beta = 4$, the overall outage probability for the interference-limited case is:

$$\mathcal{O}^{\text{SU}}(W^{\text{SU}}) = c(\kappa, \rho) \sum_{u=1}^{\infty} \frac{\Gamma^{\text{SU}}(L, u, \eta^{\text{SU}})}{B(u, \kappa - 1)} \left(\frac{1}{1 + \kappa \rho} \right)^{u-1}, \quad (6.4)$$

where $\kappa = 3.575$, $\rho = \lambda' \left(\lambda_{\text{UE}} \sum_{n \in \mathcal{F}_2} f_n \right)$, $c(\kappa, \rho) = \frac{1}{\kappa - 1} \left(\frac{\kappa}{\kappa + 1/\rho} \right)^\kappa$, $\eta^{\text{SU}} = 2^{1/W^{\text{SU}}} - 1$, $B(\cdot, \cdot)$ is the beta function defined as:

$$B(n, m) = \int_0^1 t^{n-1} (1-t)^{m-1} dt,$$

$$\Gamma^{\text{SU}}(L, u, \eta^{\text{SU}}) = \begin{cases} 1 - \sum_{l=1}^{L-u+1} \frac{(-1)^{l+1} \binom{L-u+1}{l}}{{}_2F_1\left(-\frac{1}{2}, u, \frac{1}{2}, -\eta^{\text{SU}} l \xi\right)}, & \text{for } u \leq L, \\ 1 - \frac{P_u}{{}_2F_1\left(-\frac{1}{2}, L, \frac{1}{2}, -\eta^{\text{SU}}\right)}, & \text{for } u > L \end{cases},$$

and ${}_2F_1(\cdot, \cdot, \cdot, \cdot)$ is the Gaussian hypergeometric function defined as

$${}_2F_1(a, b, c, z) = \sum_{n=0}^{\infty} \frac{(a)_n (b)_n z^n}{(c)_n n!}$$

where the coefficients are determined in terms of the Pochhammer symbols

$$(a)_n = \begin{cases} 1 & n = 0 \\ a(a+1)\dots(a+n-1) & n > 0. \end{cases}$$

For more details, see Publication P-III.

Having analyzed the outage probability of the SPUC component, we can now formulate the outage probability of the proposed hybrid scheme. The hybrid outage probability is the probability that a typical UE under service of the hybrid scheme is in outage. This gives an overall system performance that can be used to optimize the hybrid cache delivery. This is expressed as:

$$\mathcal{O}^{\text{Hyb}}(W^{\text{SU}}, W^{\text{MM}}, \mathbf{w}, \mathbf{q}) = \sum_{n \in \mathcal{F}_1} f_n \mathcal{O}_n^{\text{MM}}(W^{\text{MM}}, w_n, q_n) + \sum_{n \in \mathcal{F}_2} f_n \mathcal{O}^{\text{SU}}(W^{\text{SU}}), \quad (6.5)$$

where $\mathcal{O}_n^{\text{MM}}(W^{\text{MM}}, w_n, q_n)$ is the OMPMC outage probability for file n with service bandwidth consumption W^{MM} , and file-specific resource allocation

w_n and cache placement probability q_n . Complying with the constraint of total bandwidth consumption, we have: $\sum_{n \in \mathcal{F}_1} w_n = W^{\text{MM}}$. According to Chapter 4, for path-loss exponent $\beta = 4$, we get:

$$\mathcal{O}_n^{\text{MM}}(W^{\text{MM}}, w_n, q_n) = \text{erfc} \left(\frac{\pi^2 \lambda}{4} \frac{q_n}{\sqrt{\eta_n}} \right), \quad (6.6)$$

where $\eta_n = 2^{1/(W^{\text{MM}} w_n)} - 1$.

6.3 Optimal Hybrid Cache Policy

We consider a classifier index v to classify the files into two sets: $\mathcal{F}_1 = \{1, \dots, v\}$ and $\mathcal{F}_2 = \{v+1, \dots, N\}$. As declared, the sets \mathcal{F}_1 and \mathcal{F}_2 are served by OMPMC and SPUC, respectively. Based on the hybrid outage probability being expressed in (6.5), we thus formulate a joint constrained optimization problem. Optimization is over the classifier index v , the network-wide disjoint resources of the hybrid scheme, W^{SU} and W^{MM} , as well as over the resource allocation and the cache placement probability of the OMPMC, i.e., $\{w_n\}_{n \in \mathcal{F}_1}$ and $\{q_n\}_{n \in \mathcal{F}_1}$. The cache policy optimization problem then is:

$$(P_4): \quad \min_{\substack{W^{\text{SU}}, W^{\text{MM}} \\ \mathbf{q}, \mathbf{w}, v}} \mathcal{O}^{\text{tot}}(W^{\text{SU}}, W^{\text{MM}}, \mathbf{q}, \mathbf{w}),$$

$$\text{s.t.} \quad \begin{cases} \sum_{n=1}^v q_n = M, \quad \sum_{n=1}^v w_n = 1, \\ 0 \leq w_n \leq 1, \quad 0 \leq q_n \leq 1, \\ W^{\text{MM}} + W^{\text{SU}} = W^{\text{tot}}, \\ v \in \{0, \dots, N\}. \end{cases} \quad (6.7)$$

Problem P_4 is non-convex, in general. To find the solution, we use the Homotopy Continuation approach, discussed in Chapter 2.2, and a line search for v . As such, we formulate a parametric optimization problem exactly as P_4 but with θ -parameterized file popularity $a_n(\theta)$ replacing f_n . We denote this parametric optimization problem with $P_4(\theta)$. For $a_n(\theta)$, we need to have: $\lim_{\theta \rightarrow 0} a_n(\theta) = \frac{1}{N}$ and $\lim_{\theta \rightarrow \tau} a_n(\theta) = f_n$, where τ is the skewness of popularity distribution. The following ODEs related to P_4 can be derived:

$$\mathbf{A}(\theta) \frac{d}{d\theta} \begin{pmatrix} \mathbf{q} \\ \mathbf{w} \\ W^{\text{MM}} \\ \lambda_1 \\ \lambda_2 \end{pmatrix} = -\mathbf{b}(\theta) \quad (6.8)$$

where λ_1 and λ_2 are the Lagrange multiplier,

$\mathbf{A}(\theta) =$

$$\begin{pmatrix} [a_n(\theta)D_{q_n}^2 \mathcal{O}_n^{\text{MM}} \delta_{nm}]_{n,m} & [a_n(\theta)D_{q_n, w_n} \mathcal{O}_n^{\text{MM}} \delta_{nm}]_{n,m} & [a_n(\theta)D_{q_n, W^{\text{MM}}} \mathcal{O}_n^{\text{MM}}]_n & \mathbf{1} & \mathbf{0} \\ [a_n(\theta)D_{q_n, w_n} \mathcal{O}_n^{\text{MM}} \delta_{nm}]_{n,m} & [a_n(\theta)D_{w_n}^2 \mathcal{O}_n^{\text{MM}} \delta_{nm}]_{n,m} & [a_n(\theta)D_{w_n, W^{\text{MM}}} \mathcal{O}_n^{\text{MM}}]_n & \mathbf{0} & \mathbf{1} \\ [a_n(\theta)D_{q_n, W^{\text{MM}}} \mathcal{O}_n^{\text{MM}}]_n^\top & [a_n(\theta)D_{w_n, W^{\text{MM}}} \mathcal{O}_n^{\text{MM}}]_n^\top & \sum_{n \in \mathcal{F}_1} a_n(\theta)D_{W^{\text{MM}}}^2 \mathcal{O}_n^{\text{MM}} & 0 & 0 \\ & & + \sum_{n \in \mathcal{F}_2} a_n(\theta)D_{W^{\text{SU}}}^2 \mathcal{O}_n^{\text{SU}} & & \\ \mathbf{1}^\top & \mathbf{0}^\top & 0 & 0 & 0 \\ \mathbf{0}^\top & \mathbf{1}^\top & 0 & 0 & 0 \end{pmatrix}$$

$n, m \in \mathcal{F}_1$, $[a_{nm}]_{n,m}$ shows a matrix whose n -th row and m -th column is a_{nm} , $[a_n]_n$ is a column vector with n -th component being a_n , and

$$\mathbf{b}(\theta) = \begin{pmatrix} [\dot{a}_n(\theta)D_{q_n} \mathcal{O}_n^{\text{MM}}]_n \\ [\dot{a}_n(\theta)D_{w_n} \mathcal{O}_n^{\text{MM}}]_n \\ \sum_{n \in \mathcal{F}_1} \dot{a}_n(\theta)D_{W^{\text{MM}}} \mathcal{O}_n^{\text{MM}} - \sum_{n \in \mathcal{F}_2} \dot{a}_n(\theta)D_{W^{\text{SU}}} \mathcal{O}_n^{\text{SU}} \\ 0 \\ 0 \end{pmatrix}$$

To solve these ODEs, we need an initial condition for which we use the solution of $P_4(\theta)$ with $\theta = 0$, when the popularity is flat. This problem is expressed as: The optimum solution of $P_4(0)$ is $(q_n, w_n) = (\frac{M}{v}, \frac{1}{v})$ for $n \in \mathcal{F}_1$, where optimum value of v is obtained using a line search and a Newton-based directional approach is exploited to find optimum W^{MM} . Therefore, by solving the ODEs (6.8) with optimal initial condition of $\theta = 0$ and the target point of $\theta = \tau$, the optimal solution of P_4 can be obtained. However, we apply the prediction-correction method to numerically solve these ODEs, see Chapter 2.2 for more information.

6.4 Simulation Results

In this section, we compare the optimal cache solution of the hybrid scheme to the conventional multi-antennas SPUC scheme [19, 42, 43] and OMPMC scheme investigated in Chapters 4 and 5.

The following scenario is considered for the benchmark: The number of files is $N = 100$, the popularity skewness is $\theta = 0.6$, the cache capacity of BSs is $M = 10$, the total bandwidth of the network is $W^{\text{tot}} = 15$ in units $[\frac{\text{Hz}}{\text{bits/s}}]$ and $L = \{2, 4, 8\}$ antennas at the BSs. The intensity of BSs is $\lambda = 10$ and intensity of UEs varies in the range $\lambda_{\text{UE}} \in [10, 100]$. We consider a reference SNR $\gamma_{\text{tx}} = 1$, which corresponds to an environment with carrier frequency equal to 2 GHz, reference distance equal to 1 km, BSs transmit

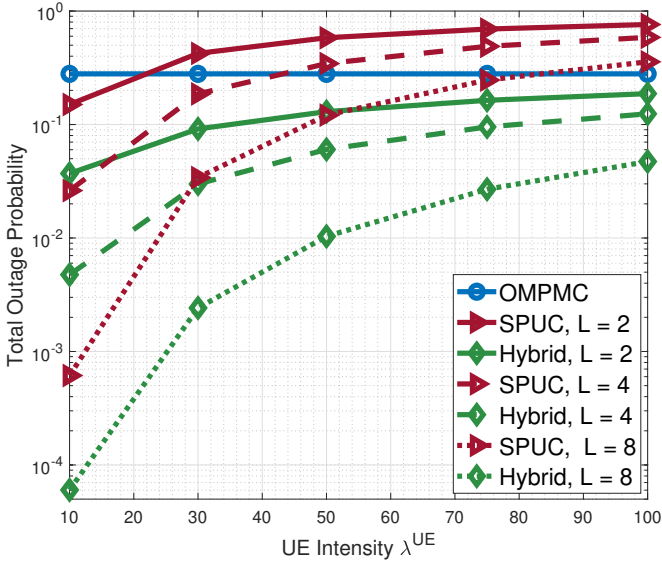


Figure 6.1. The total outage probability as a function of the UE intensity λ_{UE} .

power 23 dBm, the sum of antenna gains at the BS and UE equal to 9 dBi, and the UE noise figure 9 dB. Note that since the reference distance is 1 km, the UE and BS intensities are in the units of points/km².

In Figure 6.1, the total outage probability is plotted as a function of the UE intensity λ_{UE} . The hybrid scheme outperforms other policies for all evaluated UE intensities and numbers of antennas. Notice that the OMPMC scheme is insensitive to the UE intensity and to the number of BS antennas. Although OMPMC outperforms the SPUC schemes for large UE intensities, the hybrid scheme remains superior to the OMPMC also for those intensities. As the UE intensity grows, the gap between the OMPMC and the hybrid scheme decreases. The reason is that some UEs that prefers less popular files are not served at all by the network. As the number of antennas increases, the performance gap between the hybrid and the SPUC schemes grows.

To study how the hybrid scheme allocates resources between OMPMC and SPUC, the bandwidth ratio W^{SU}/W^{tot} is shown in Figure 6.2 as a function of the UE intensity λ_{UE} . As the UE intensity increases, resources are allocated to SPUC. Considering the insensitivity of OMPMC to UE intensity, the reason is that the SPUC part needs more resources to optimize the total outage probability as the number of requesting UEs grows. When the number of antennas increases, the resource reserved for the SPUC part decreases, as SPUC is then able to fulfill more UEs in each cell per resource.

We use the ratio v/N of the threshold to the total number of files, to

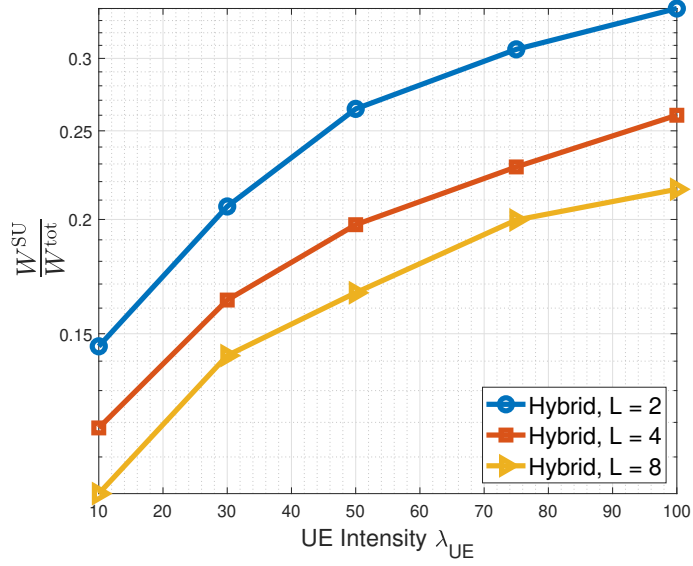


Figure 6.2. The resource allocation ratio as a function of the UE intensity λ_{UE} .

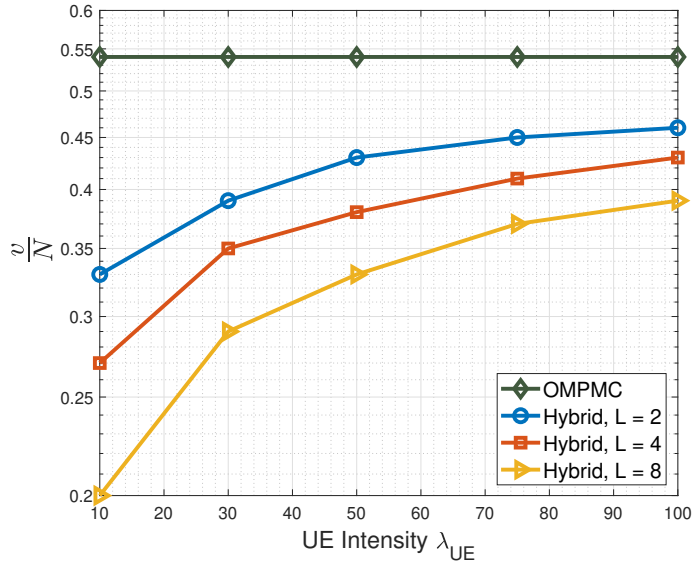


Figure 6.3. The file classification ratio as a function of the UE intensity λ_{UE} .

investigate how the files are classified into \mathcal{F}_1 and \mathcal{F}_2 for the hybrid scheme as a function of the UE intensity λ_{UE} . Figure 3 shows that as UE intensity increases more files are cached at the BSs and offloaded to the OMPMC component. The reason is that as the UE intensity grows, the outage probability of the SPUC component increases. As the number of antenna increases at the BSs, more UEs can be served by the SPUC component.

6.5 Conclusion

In this chapter, we considered file delivery in a cellular system based on a hybrid scheme combining caching-based multicast and on-demand unicast service. We classified the files into sets of popular and less popular ones. Files of the popular set were cached at BSs and delivered by OMPMC, simultaneously available to all users in the network who are interested in those files. The less popular set is delivered by on-demand SPUC transmissions. A closed-form expression was obtained for the total outage probability of the hybrid scheme based on stochastic geometry analysis. The cache policy was formulated based on a time-varying optimization problem and the hybrid scheme was jointly optimized based on the caching placement, resource allocation and file classification. We compared the performance of the proposed compound scheme with the SPUC and OMPMC approaches from the literature. Simulation results showed that the outage probability of the hybrid scheme outperforms other caching strategies for different user intensities and number of antennas. As a future work, the usage of a size-biased Gamma distribution, evaluating the difference with respect to the current cache solution and result comparison can be considered.

7. Dynamic Cache Policy Design using Reinforcement Learning

In the previous chapters, we studied and designed static cache policies being optimized for a time-slot operation of cellular networks. In this chapter, by contrast, we consider the dynamics of cellular networks during different time-slots, and design an optimal dynamic cache policy. This chapter is based on Publication P-IV. The probabilistic content placement and OMPMC delivery scheme, as introduced in Chapter 3.2 and 3.3, are considered for cellular networks. In addition, users may store files in their UE caches. We then consider an RL-based cache policy for cellular networks and model the dynamics of UE file preferences by a Markov process. The cache policy is designed by taking into account the user Quality of Service and the backhaul load, and using the Advantageous Actor-Critic RL framework with two neural networks.

Section 7.1 is devoted to explaining the dynamics and timing model of network operation. In Section 7.2, a dynamic cache policy is formulated based on a MDP, and is optimized using the A2C algorithm. We benchmark the performance of the proposed RL-based cache policy and compare its performance with the policies from the literature, in Section 7.3.

7.1 Timing Model of Network Operation

In this chapter, a cellular network with an associated core network is considered. BSs fetch files from the core network via error-free backhaul links. Both UEs and BSs are equipped with independent storage-limited caches that store files according to the probabilistic model described in Chapter 3.3. UEs choose files based on file preferences. If a UE chooses a file that is stored in its cache, it can directly obtain it, if it is not locally cached, the UE requests the file from the network. Based on the aggregate requests from the UEs, the network updates BS caches, and transmit the files over the air interface. The UEs and BSs are deployed based on two independent PPPs. Changes in file preferences, file requests by UEs, file fetching by BSs from the core network, and file delivery towards UEs are

modeled on a per-slot basis, with slots indexed by t .

7.1.1 File Popularity and User Requests

In each time-slot, UEs choose files from a library \mathcal{F} containing N files. The popularity of file n at time-slot t is $p_n(t) \in [0, 1]$. This distribution is not assumed to be a priori known, it emerges from the aggregate UE behavior at time-slot t . For simulations, a Zipf distribution, described in Chapter 3.2, is used to model file popularity, $p_n(t) = n^{-\tau(t)} / \sum_{j=1}^N j^{-\tau(t)}$ for $j = 1, \dots, N$, where $\tau(t)$ stands for the skewness at time-slot t . File popularity evolves based on a finite state Markov chain [52] with M states and state set $\mathcal{Q} := \{Q_1, \dots, Q_M\}$. The unknown transition probability matrix is denoted by \mathbf{Q} .

In this work, the popularity distribution is unknown for the network, and network optimization is based on the realized requests of UEs in different time slots. The considered cache policy is thus agnostic to the file popularity model.

Caching of files at UEs is based on a probabilistic method. The UE cache probability $s_n(t)$ determines the probability that file n is stored at a UE cache in time-slot t . We assume that the cache of each UE has maximum capacity L_u , i.e., $\sum_{n=1}^N s_n(t) \leq L_u$. A UE preferring a file only requests it from the network if the file has not been stored at its cache. Accordingly, the probability that a given UE requests a file at time-slot t becomes

$$\mathbf{r}^{\text{net}}(t) = \mathbf{p}(t) \odot (\mathbf{1} - \mathbf{s}(t)), \quad (7.1)$$

this is a vector with one entry per file, $\mathbf{r}^{\text{net}}(t) = [r_1^{\text{net}}(t), \dots, r_N^{\text{net}}(t)]^\top$, and $\mathbf{s}(t) = [s_1(t), \dots, s_N(t)]^\top$ is a vector of the UE caching probabilities, $\mathbf{p}(t) = [p_1(t), \dots, p_N(t)]^\top$ is a vector of file popularities, and $\mathbf{1}$ is an N -dimensional vector with all elements being one. The file request probability decreases with increasing UE caching probability, and grows with increasing file popularity.

7.1.2 Cache Placement

Based on the probabilistic model of BSs caching, an overall cache probability vector is considered: $\boldsymbol{\rho}(t) = [\rho_1(t), \dots, \rho_N(t)]^\top$, see Chapter 3.3. Complying with the cache capacity, we have: $\sum_{n=1}^N \rho_n(t) \leq L_c$.

7.1.3 Cache Delivery

After updating the caches of BSs, files are broadcasted towards the UEs in dedicated resources $w_n(t)$, using OMPMC scheme, explained in Chapters 3.5. If the SNR associated to a file at a requesting UE is less than a threshold, the request will be in outage. The outage probability depends on the caching probability $\boldsymbol{\rho}(t)$ and allocated resource $\mathbf{w}(t)$.

The outage probability of the OMPMC network is analyzed in Chapter 4. As such, for an environment with path-loss exponent $\beta = 4$, BSs with intensity λ , file n being cached with probability $\rho_n(t)$ and being allocated with bandwidth $w_n(t)$, the outage probability for this file is:

$$\mathcal{O}_n(t) = \text{erfc} \left(\frac{\pi^2 \lambda \rho_n(t)}{4 \sqrt{\eta_n(t)}} \right), \quad (7.2)$$

where $\eta_n(t) = \frac{1}{\gamma_{\text{tx}}} (2^{\alpha/w_n(t)} - 1)$ is the channel gain threshold being expressed in terms of a spectral efficiency threshold α .

7.1.4 UE Cache Policy

The cache probability of the UEs for the next time-slot depends on the current caching probability and the outage probability. The files already cached, and the files that the UE can decode, are candidates for caching. If the number of candidate files exceeds the UE cache capacity L_u , the UE chooses L_u files among the candidates uniformly at random. On the population level, this leads to the caching probability update equation

$$\begin{aligned} \tilde{\mathbf{s}}(t+1) &= \mathbf{s}(t) + (\mathbf{1} - \mathbf{s}(t)) \odot (\mathbf{1} - \mathcal{O}(t)), \\ \mathbf{s}(t+1) &= \min \left\{ 1, \frac{L_u}{\sum_{n=1}^N \tilde{s}_n(t+1)} \right\} \tilde{\mathbf{s}}(t+1), \end{aligned} \quad (7.3)$$

where $\mathcal{O}(t) = [\mathcal{O}_1(t), \dots, \mathcal{O}_N(t)]^\top$.

7.1.5 Overall View of Network Operation

In equations (7.1)-(7.3), the problem was formulated based on probabilistic vectors $\mathbf{r}^{\text{net}}(t)$, $\mathbf{s}(t)$ and $\boldsymbol{\rho}(t)$ instead of vectors related to individual users and BSs. Thus, the cache policy update during time-slot t consists of three consecutive phases: the request announcement, cache update and placement and the cache delivery. The interactions between UEs, BSs and the core network during time-slot t are illustrated in Figure 7.1.

7.2 RL-based Dynamic Cache Policy

To find a dynamic optimal cache policy, we use the RL-based A2C algorithm, described in Chapter 2.3. As such, we need to define the system state and action vectors, as well as the structure of actor and critic networks should be specified. In the followings, we first set the state and action vectors, and correspondingly formulate a dynamics-aware optimization problem. Then, we specify the actor and critic networks that are used in the A2C algorithm. At the end, we present a RL-based cache policy algorithm.

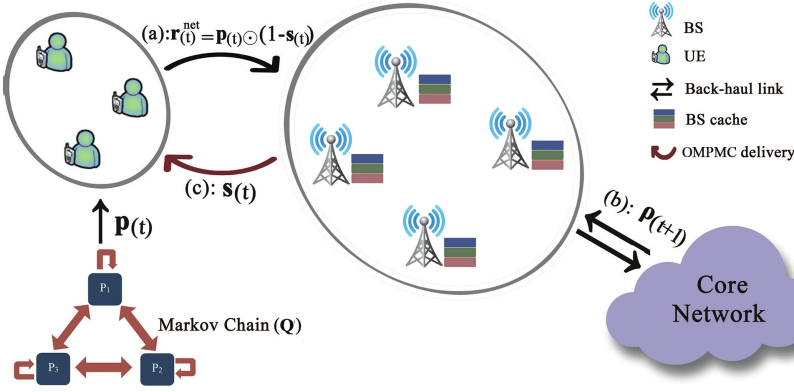


Figure 7.1. The interactions between UEs, BSs and core network for CPD policy. Phase (a): UEs requests. Phase (b): BSs fetch files from the core network and update their caches. Phase (c): OMPMC cache delivery and update of UEs caches.

7.2.1 Problem Formulation

Users request files based on their preference and cache status. Therefore, the system state vector is constituted based on the file request probability (7.1) and the UE cache probability (7.3).

$$\mathbf{x}(t) = [\mathbf{r}^{\text{net}}(t)^\top, \mathbf{s}(t)^\top]^\top. \quad (7.4)$$

The feasible set for the state vector is

$$\mathcal{X} = \mathcal{R} \times \mathcal{S}, \quad (7.5)$$

where $\mathcal{S} = \{\mathbf{s} \mid \mathbf{s} \geq \mathbf{0}, \mathbf{1}^\top \mathbf{s} \leq L_u\}$, and $\mathcal{R} = \{\mathbf{r} \mid \mathbf{r} \geq \mathbf{0}, \mathbf{1}^\top \mathbf{r} \leq 1\}$. The network action vector is constituted by the cache probability of BSs and the allocated resources:

$$\mathbf{u}(t) = [\boldsymbol{\rho}(t)^\top, \mathbf{w}(t)^\top]^\top. \quad (7.6)$$

The feasible set of actions is constrained by the capacity of BS caches and the total available bandwidth:

$$\mathcal{U} = \{(\boldsymbol{\rho}, \mathbf{w}) \mid \boldsymbol{\rho} \geq \mathbf{0}, \mathbf{1}^\top \boldsymbol{\rho} \leq L_c, \mathbf{w} \in [0, 1]^N, \mathbf{1}^\top \mathbf{w} = 1\}. \quad (7.7)$$

In this chapter, we are interested in high QoS achieved with small back-haul load. The availability probability of preferred files at UEs is considered as a measure of QoS. For this, the probability that a requesting UE gets the file from the network is considered. Considering all files, the reward should be averaged over the file popularity. This QoS reward function is expressed in terms of the request probability (7.1) and the outage

probability (7.2) as:

$$\begin{aligned} r_{\text{QoS}}(t) &= 1 - \sum_{n=1}^N p_n(t) [s_n(t) + (1 - s_n(t))(1 - \mathcal{O}_n(t))] \\ &= 1 - \sum_{n=1}^N r_n^{\text{net}}(t) \mathcal{O}_n(t). \end{aligned} \quad (7.8)$$

For more details about (7.8), see Publication P-IV.

The backhaul load is related to the number of files fetched from the core network. If $\rho_n(t) - \rho_n(t-1) \leq 0$, no BS needs to fetch file n in time-slot t , and only some BSs may have to delete the file from their cache. If $\rho_n(t) - \rho_n(t-1) > 0$, a corresponding fraction of BS have to fetch the file, using the backhaul network. The probability that a BS has to fetch file n is thus given by $[\rho_n(t) - \rho_n(t-1)]_+$, where $[x]_+ = \frac{1}{2}(x + \text{abs}(x))$. Hence, the aggregate backhaul reward is shaped as

$$r_{\text{bh}}(t) = L_c - \sum_{n=1}^N [\rho_n(t) - \rho_n(t-1)]_+. \quad (7.9)$$

A joint optimization problem can be formulated based on the costs of backhaul and QoS as:

$$r(t) = r_{\text{QoS}}(t) + \lambda_{\text{bh}} r_{\text{bh}}(t), \quad (7.10)$$

where λ_{bh} regulates between user satisfaction and backhaul load. A discounted average reward starting from time-slot t till time horizon T can then be defined as:

$$R(t) = \sum_{k=t}^T \gamma^{k-t} \mathbb{E}[r(k)], \quad (7.11)$$

where T is number of time-slots in the caching process and $\gamma \in [0, 1]$ is the discount factor.

We are interested in maximizing $R(t)$ starting from any time-slot t . The cache policy design is thus formulated as a constrained optimization problem:

$$\begin{aligned} P_{\text{RL}} : \quad & \max_{\pi(\cdot|\mathbf{x}(t))} R(t), \quad 0 \leq t \leq T \\ \text{s.t.} \quad & \begin{cases} \mathbf{u}(k) \sim \pi(\cdot|\mathbf{x}(t)) \in \mathcal{U}, \quad \text{for } k \geq t \\ (7.1) - (7.3), (7.8) - (7.11). \end{cases} \end{aligned} \quad (7.12)$$

where $\pi(\cdot|\mathbf{x}(t))$ denotes the policy distribution by which the action $\mathbf{u}(t)$ are generated given state $\mathbf{x}(t)$. The aim is thus to learn a policy $\pi(\cdot|\mathbf{x}(t))$ which maximizes $R(t)$ starting from any time-slot t .

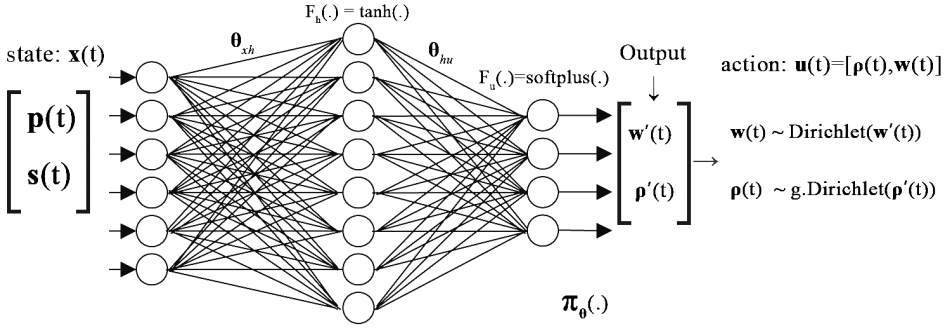


Figure 7.2. The structure of the actor neural network $\pi_{\theta}(\cdot)$.

7.2.2 Structure of Actor and Critic Networks

The actor and critic agents are designed using two separate neural networks. One hidden layer is used for the ϕ -parameterized critic network and the rectified linear unit (ReLU) activation function is used for each neuron. The critic network is leveraged to criticize the actor performance by generating the Value-function, and based on the process described in Chapter 2.3.

Figure 7.2 depicts the structure of the θ -parameterized actor network. It has one hidden layer with hyperbolic tangent activation functions. The output layer is acted on by a *softplus* function. The standard actor network of the A2C considers a Gaussian distribution to generate the action vector. However, to enforce the constraints (7.7) over the action vector, we modify the actor network and consider Dirichlet distributions to generate the action vector as:

$$\mathbf{u}(t) \sim \begin{bmatrix} L_c \cdot \text{Dirichlet}(\boldsymbol{\rho}'(t, \boldsymbol{\theta})) \\ \text{Dirichlet}(\mathbf{w}'(t, \boldsymbol{\theta})) \end{bmatrix},$$

where $\boldsymbol{\rho}'(t, \boldsymbol{\theta})$ and $\mathbf{w}'(t, \boldsymbol{\theta})$ are the outputs of the θ -parameterized actor network, and $\text{Dirichlet}(\cdot)$ stands for the multivariate Dirichlet distribution. Considering that the elements of any random vector generated from a Dirichlet distribution lie between zero and one, and the sum of its elements equals to one, the constraints of (7.7) are implicitly enforced.

It is noteworthy that we use the procedure described in Chapter 2.3, equation (2.5) to update the critic and actor networks.

7.2.3 RL-based Cache Policy Algorithm

Algorithm 4 shows the pseudo code for the proposed RL-based cache policy based on modified A2C. In the pseudo-code, E_{\max} stands for the maximum number of episodes for which the training process is performed and N_u is the number of time-slots after which the actor and critic networks

Algorithm 4 The Modified A2C for Cache policy design.

```

1: for  $episode = 1$  to  $E_{\max}$  do
2:   Given the initial system state vector  $\mathbf{x}(1)$ , actor and critic networks
   parameterized with  $\theta$  and  $\phi$ .
3:   for  $t = 1$  to  $T$  do
4:     Select an action  $\mathbf{u}(t)$  following  $\pi_{\theta}(\cdot|\mathbf{x}(t))$  and interact with the envi-
     ronment.
5:     Critic network provides estimate of value-function  $V_{\phi}(\mathbf{x}(t))$ .
6:     Observe new state  $\mathbf{x}(t+1)$  and immediate reward  $r(t)$ .
7:     Buffer  $V_{\phi}(\mathbf{x}(t))$ ,  $\mathbf{x}(t)$ ,  $r(t)$ ,  $\log(\pi_{\theta}(\mathbf{u}(t)|\mathbf{x}(t)))$ , and  $H(\pi_{\theta}(\mathbf{u}(t)|\mathbf{x}(t)))$ .
8:     Update parameters of actor and critic networks as in (2.5) every
      $N_u$  time-slot.
9:   end for
10: end for

```

are updated.

7.3 Simulation Results

In this section, we compare the proposed RL-based dynamic policy to the optimal method, as well as to two cache schemes from the literature [3], namely, "Least Recently Used" (LRU) and "Least Frequently Used" (LFU) strategies. LRU policy is formulated based on tracking the most recent request and removing the least recently used file from the cache when it is full, while LFU strategy is formulated based on keeping the most frequently requested files in the cache of BSs. To find the optimal method, we use the interior-point algorithm to solve the optimization problem.

The following scenario is taken into account for the benchmark. A cellular network with cache-equipped BSs is considered. The intensity and average transmission power of BSs are $\lambda = 50$ and $\bar{p} = 1$, respectively. The UE noise power is $\sigma_0^2 = 1$ and the spectral efficiency threshold is $\alpha = 1/5$. As [57, 74], we consider a Markov process to model the preference profile. The popularity profile is thus modeled by a four-state Markov chain with transition matrix

$$\mathbf{Q} = \begin{pmatrix} 0.9 & 0.033 & 0.033 & 0.033 \\ 0.2 & 0.7 & 0.05 & 0.05 \\ 0.05 & 0.05 & 0.85 & 0.05 \\ 0.1 & 0.1 & 0.1 & 0.7 \end{pmatrix}, \quad (7.13)$$

and the corresponding state set contains Zipf distributions with skewness values $\tau = \{2, 2.5, 3, 3.5\}$. We set $N = 40$ files in the library, the capacity of BSs caches are $L_c = 6$, and the capacity of UEs caches are $L_u = 3$. The total

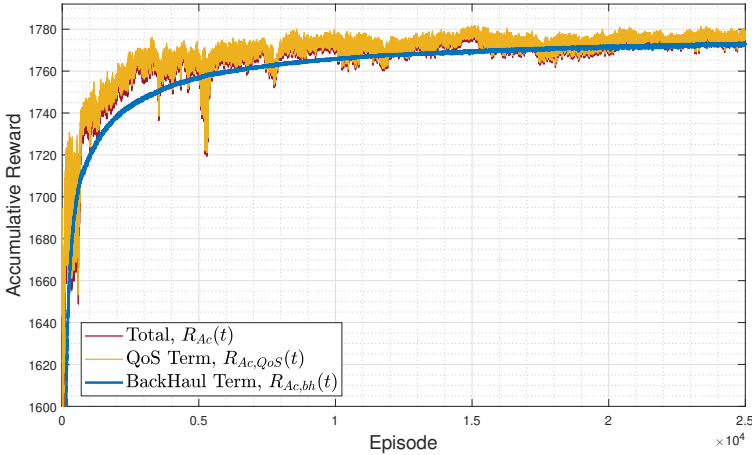


Figure 7.3. Training performance of the RL agent in term of the accumulative reward.

number of time-slots is $T = 256$.

For the A2C algorithm, the hyperparameters are tuned as follows. For the actor and critic networks, the number of neurons in the hidden layer is 64. We observed that increasing the number of neurons does not give better performance in terms of accumulative reward, while it needs more data for tuning the parameters of the networks. We also set $E_{\max} = 2.5 \times 10^4$ and $N_u = 128$. We use $\lambda_{bh} = 0.05$ to regulate the cost of backhaul, $\gamma = 0.98$ for the discount factor and $\beta_{ent} = 10^{-2}$ for regularization of the entropy term. The learning rates of the actor and critic networks are $\psi = 7 \times 10^{-3}$ and $\delta = 7 \times 10^{-3}$.

Figure 7.3 shows the training performance of the proposed dynamic policy in terms of the accumulative reward $R_{Ac}(t) = \sum_{k=1}^t r(k)$, and QoS and backhaul terms of accumulative reward, i.e., $R_{Ac, QoS}(t) = \sum_{k=1}^t r_{QoS}(k)$ and $R_{Ac, bh}(t) = \sum_{k=1}^t r_{bh}(k)$. As this figure illustrates, the RL-based policy is trained after approximately 1.5×10^4 episodes for the aforementioned cellular network parameters.

Figure 7.4 shows the comparison of test performance between RL-based policy, LRU, LFU and "Optimum" for 128 Episodes in term of the accumulative reward. As this figure shows, the performance of the RL-based policy outperforms other cache policy approaches. The "Optimum" policy slightly outperforms RL-based policy, at a considerable complexity cost.

The experimental CDF of the instantaneous QoS reward (7.8) across time-slots is plotted in Figure 7.5. This shows the statistics of QoS experienced by UEs during the network dynamics after the agent is fully trained. Note that the instantaneous QoS reward indicates the probability that a user gets the needed file. The closer it is to one, the more probable it is that users have either cached, or have successfully received their files of interest in a given slot. For the RL-based and "Optimum" policies, the CDF

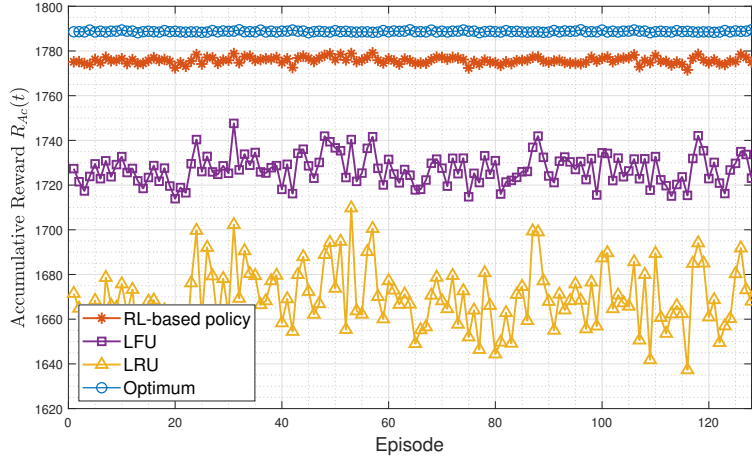


Figure 7.4. Performance comparison between the RL-based CPD, LFU, LRU and "Optimum" cache policies in term of the accumulative reward.

is aggregated on values greater than 0.9, meaning that users are satisfied with high probability. However, for the LRU and LFU policies the CDF is distributed over a greater range meaning that in some slots the network fails to fulfil user requests.

The experimental CDF corresponding to the instantaneous backhaul reward (7.9), is sketched in Figure 7.6. The smaller it is, the more costly it is to fetch the files from the core network. For the RL-based and "Optimum" policies, the CDF is concentrated near the maximum reward $L_c = 6$, implying that in each time-slot these policies have proactively cached at BSs most files that will be requested by UEs in the next time-slot, and the network will not need to fetch many files. However, for the LRU and LFU policies, the files fail to be cached at BSs proportional to user requests which causes backhaul load for the network.

7.4 Conclusion

In this chapter, we formulated the cache policy design based on a reinforcement learning framework. We shaped a reward function aiming to optimize the user QoS and backhaul load. We utilized an A2C algorithm and neural networks to learn an optimal dynamic cache policy. Simulation results showed that the proposed RL-based method outperforms other caching approaches and at the same time its difference with the optimum method is negligible.

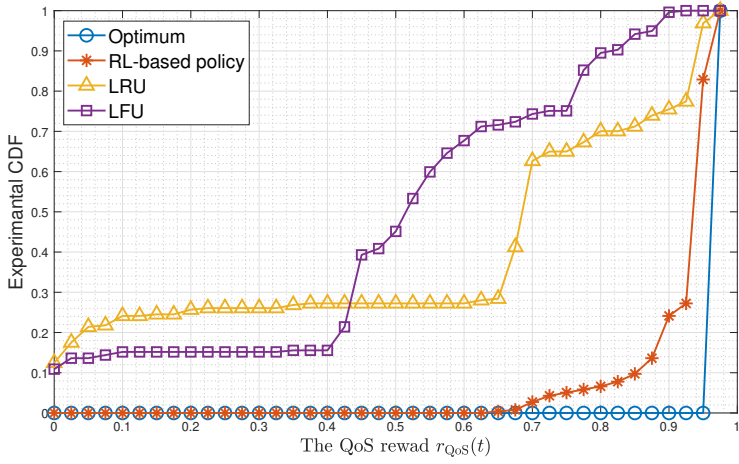


Figure 7.5. Experimental CDF of the QoS reward during network dynamics.

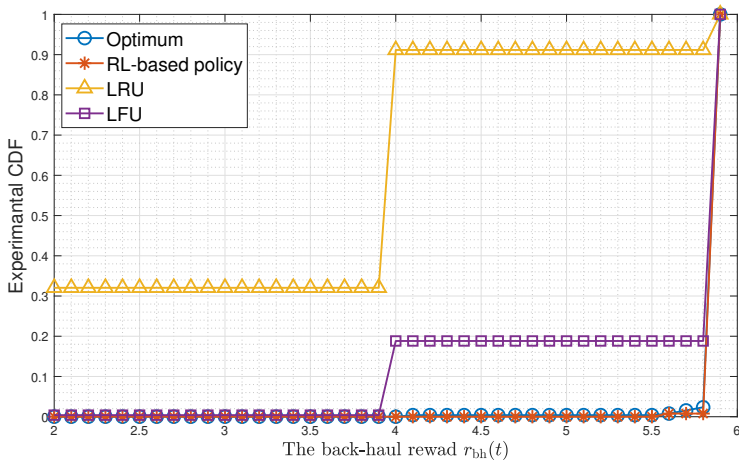


Figure 7.6. Experimental CDF of the backhaul reward during network dynamics.

8. Conclusion and Future Work

Edge caching is a promising approach to cope with the unprecedented data congestion and traffic escalation issues of mobile cellular networks. To design an optimal cache strategy, the two phases of cache placement and cache delivery should be taken into account. On the other hand, considering the model of network operation, a cache policy can be designed in a static or dynamic framework.

In the line with static framework, we focused on optimizing the cache placement and content delivery scheme. As such, we considered the orthogonal multipoint multicast transmission accompanied by a probabilistic cache placement. To control the performance of placement and delivery phases, cache probabilities and resource-allocation parameters were introduced. An expression was obtained and analyzed for the overall outage probability as a network performance. An algorithm was then devised to find the optimal cache solution, based on a formulated constrained optimization problem. Due to its computational complexity, we also devised a low-complexity algorithm by relaxation trick which enabled us to find the solution with a negligible relaxation gap. As such, the cache solution was characterized by a file popularity threshold, with files less popular not being cached nor delivered at all.

We found that using the OMPMC scheme in cache-enabled networks can promisingly improve the spectral-efficiency of the whole network, compared to a single-point transmission scheme. We further evaluated the effect of ICI and IBI on the optimal OMPMC cache policy in the cache-enabled cellular networks. We found that considering the ICI/IBI in caching optimization provides systematically better results than neglecting it. However, for a long Cyclic Prefix (CP), ICI/IBI can be neglected without degrading the performance of the cache policy. This shows that for the long CP, the cache solution being obtained with neglecting the ICI/IBI still is valid and can be considered to evaluate the performance of OMPMC scheme for the cellular networks.

Inspired by the result of the MPMC cache policy that *the most popular files are only cached*, a hybrid scheme based on MPMC and multi-antenna

single-point unicast (SPUC) was considered in the context of the static caching framework. The most popular files are cached at the BSs and served by OMPMC, whereas the remaining files are fetched from the core network on demand and served by SPUC. A closed-form expression was derived for the total outage probability based on which a time-varying optimization problem was formulated to find the optimal cache solution. Based on the results, we realized that the hybrid scheme can outperform MPMC and SPUC caching strategies for different user intensities and the number of antennas. The reason can be explained as follow. The MPMC is more efficient to be exploited for the networks with considerable UEs interested in files with high popularity. The usage of MPMC for less popular files wastes the resources of the network, compared to the usage of SPUC. As such, classifying the files into low- and high-popularity files, using the multicast resources only for the high popular files, and serving the remaining files with on-demand SPUC remarkably improve network performance. This shows that incorporating OMPMC-based caching in a conventional SPUC cellular network, and operating the network following the proposed hybrid scheme is a promising content delivery approach for future wireless networks.

In the line with dynamic framework, the user requests in cellular networks was modeled based on a Markov Decision Process (MDP). The Quality-of-Service and backhaul load were considered as rewards for designing a dynamic cache strategy. As such, a constrained optimization problem was formulated with respect to a stochastic cache policy and based on an accumulative discounted reward function. We used the A2C algorithm to find the optimal cache solution. We found that the proposed RL-based cache method outperforms other dynamic caching from the literature and at the same time its difference from the optimum method is negligible.

Whether static or dynamic cache policy, the caching policies throughout this thesis are designed in a centralized framework. As such, it is of interest to study the dynamic and static cache policy design based on the distributed approaches considering the communication burden and physical-layer impairments.

References

- [1] Cisco Annual Internet Report White Paper. *Cisco, Technology Report*, Mar. 2020.
- [2] 3GPP. Universal mobile telecommunications system (UMTS); radio frequency RF system scenarios. Technical report (TR), 3rd Generation Partnership Project (3GPP), April 2017. Version 14.0.0.
- [3] Mohamed Ahmed, Stefano Traverso, Paolo Giaccone, Emilio Leonardi, and Saverio Niccolini. Analyzing the performance of LRU caches under non-stationary traffic patterns. preprint ArXiv 1301.4909v1, jan. 2016.
- [4] Eugene L. Allgower and Kurt Georg. *Introduction to Numerical Continuation Methods*. Society for Industrial and Applied Mathematics, 2003.
- [5] Simonetto Andrea, Mokhtari Aryan, Koppel Alec, Leus Geert, and Alejandro Ribeiro. A class of prediction-correction methods for time-varying convex optimization. *IEEE Transactions on Signal Processing*, 64(17):4576–4591, 2016.
- [6] Jeffrey G. Andrews, Francois Baccelli, and Radha Krishna Ganti. A tractable approach to coverage and rate in cellular networks. *IEEE Transactions on Communications*, 59(11):3122–3134, 2011.
- [7] Jeffrey G. Andrews, Abhishek K. Gupta, and Harpreet S. Dhillon. A primer on cellular network analysis using stochastic geometry. preprint ArXiv 1604.03183, Apr. 2016.
- [8] Francois Baccelli and Bartłomiej Błaszczyszyn. Stochastic geometry and wireless networks, volume i: Theory. *Found. Trends Netw.*, 3(3-4):249–449, 2009.
- [9] Francois Baccelli and Bartłomiej Błaszczyszyn. Stochastic geometry and wireless networks, volume ii: Applications. *Found. Trends Netw.*, 3(3-4):249–449, 2009.
- [10] Ejder Bastug, Mehdi Bennis, and Mérouane Debbah. Living on the edge: The role of proactive caching in 5G wireless networks. *IEEE Communications Magazine*, 52(8):82–89, August 2014.
- [11] Michel Batarieri, Kevin Baum, and Thomas P. Krauss. Cyclic prefix length analysis for 4G OFDM systems. In *IEEE Vehicular Technology Conference (VTC)*, volume 1, pages 543–547, September 2004.
- [12] Mozghan Bayat, Ratheesh Mungara, and Giuseppe Caire. Achieving spatial scalability for coded caching via coded multipoint multicasting. *IEEE Transactions on Wireless Communications*, 18(1):227–240, January 2019.

- [13] Yoshua Bengio, Aaron C. Courville, and Pascal Vincent. Unsupervised feature learning and deep learning: A review and new perspectives. preprint arXiv 1206.5538, 2012.
- [14] Bartłomiej Blaszczyszyn and Anastasios Giovanidis. Optimal geographic caching in cellular networks. In *IEEE International Conference on Communications (ICC)*, pages 3358–3363, June 2015.
- [15] Stephen Boyd and Lieven Vandenbergh. *Convex Optimization*. Cambridge, U.K.: Cambridge Univ. Press, 2004.
- [16] Lee Breslau, Pei Cao, Li Fan, Graham Phillips, and Scott Shenker. Web caching and Zipf-like distributions: Evidence and implications. In *IEEE International Conference on Computer Communications, (INFOCOM)*, pages 126–134, 1999.
- [17] Dongxu Cao, Sheng Zhou, and Zhisheng Niu. Optimal base station density for energy-efficient heterogeneous cellular networks. In *IEEE International Conference on Communications (ICC)*, pages 4379–4383, June 2012.
- [18] Youjia Chen, Ming Ding, Jun Li, Zihuai Lin, Guoqiang Mao, and Lajos Hanzo. Probabilistic small-cell caching: Performance analysis and optimization. *IEEE Transactions on Vehicular Technology*, 66(5):4341–4354, 2017.
- [19] Zheng Chen, Ling Qiu, and Xiaowen Liang. Area spectral efficiency analysis and energy consumption minimization in multi-antenna Poisson distributed networks. *IEEE Transactions on Wireless Communications*, 15(7):4862–4874, 2016.
- [20] Fen Cheng, Guan Gui, Nan Zhao, Yunfei Chen, Jie Tang, and Hikmet Sari. UAV-relaying-assisted secure transmission with caching. *IEEE Transactions on Communications*, 67(5):3140–3153, 2019.
- [21] Minseok Choi, Andreas F. Molisch, Dong-Jun Han, Dongjae Kim, Joongheon Kim, and Jaekyun Moon. Probabilistic caching and dynamic delivery policies for categorized contents and consecutive user demands. *IEEE Transactions on Wireless Communications*, 20(4):2685–2699, 2021.
- [22] Ying Cui and Dongdong Jiang. Analysis and optimization of caching and multicasting in large-scale cache-enabled heterogeneous wireless networks. *IEEE Transactions on Wireless Communications*, 16(1):250–264, Jan. 2017.
- [23] Daryl J. Daley and David Vere-Jones. *An Introduction to the Theory of Point Processes: Volume II: General Theory and Structure*. Springer, 2007.
- [24] Peter Deufhard. *Newton Methods for Nonlinear Problems: Affine Invariance and Adaptive Algorithms*. Springer, New York, 2011.
- [25] Harpreet S. Dhillon, Radha Krishna Ganti, Francois Baccelli, and Jeffrey G. Andrews. Modeling and analysis of K-tier downlink heterogeneous cellular networks. *IEEE Journal on Selected Areas in Communications*, 30(3):550–560, 2012.
- [26] Ericsson. Energy and carbon report. *White paper*, Nov. 2014.
- [27] Mahyar Fazlyab, Santiago Paternain, Victor M. Preciado, and Alejandro Ribeiro. Prediction-correction interior-point method for time-varying convex optimization. *IEEE Transactions on Automatic Control*, 63(7):1973–1986, 2018.
- [28] Navneet Garg, Mathini Sellathurai, Bharath Bettagere, Vimal Bhatia, and Tharmalingam Ratnarajah. Online learning models for content popularity prediction in wireless edge caching. In *Asilomar Conf. Signals, Syst., Comput.*, pages 337–341, 2019.

- [29] Phillipa Gill, Martin Arlitt, Zongpeng Li, and Anirban Mahanti. Youtube traffic characterization: a view from the edge. In *ACM SIGCOMM*, 2007.
- [30] Anastasios Giovanidis and Bartłomiej Błaszczyszyn. Randomised geographic caching and its applications in wireless networks. 2021.
- [31] Andrea Goldsmith. *Wireless Communications*. Cambridge University Press, 2005.
- [32] Ivo Grondman, Lucian Busoniu, Gabriel A. D. Lopes, and Robert Babuska. A survey of actor-critic reinforcement learning: Standard and natural policy gradients. *IEEE Transactoin on Systems, Man, and Cybernetics, Part C (Applications and Reviews)*, 42(6):1291–1307, 2012.
- [33] Martin Haenggi and Radha Ganti. Interference in large wireless networks. *Found. Trends Netw.*, 3:127–248, 01 2009.
- [34] Nihar Jindal, Jeffrey G. Andrews, and Steven Weber. Multi-antenna communication in ad hoc networks: Achieving MIMO gains with SIMO transmission. *IEEE Transactoins on Communications*, 59(2):529–540, 2011.
- [35] Han-Shin Jo, Young Jin Sang, Ping Xia, and Jeffrey G. Andrews. Heterogeneous cellular networks with flexible cell association: A comprehensive downlink SINR analysis. *IEEE Transactions on Wireless Communications*, 11(10):3484–3495, 2012.
- [36] J. Kingman. *Poisson Processes*. Oxford, England: Oxford University Press, 1993.
- [37] Harshat Kumar, Alec Koppel, and Alejandro Ribeiro. On the sample complexity of Actor-Critic for reinforcement learning. *Conference on Neural Information Processing Systems (NeurIPS)*, 2019.
- [38] Vyacheslav Kungurtsev and Moritz Diehl. Sequential quadratic programming methods for parametric nonlinear optimization. *Computational Optimization and Applications*, 59(3):475–509, February 2014.
- [39] Namyoon Lee, David Morales-Jimenez, Angel Lozano, and Robert W. Heath. Spectral efficiency of dynamic coordinated beamforming: A stochastic geometry approach. *IEEE Transactions on Wireless Communications*, 14(1):230–241, 2015.
- [40] Kuikui Li, Chenchen Yang, Zhiyong Chen, and Meixia Tao. Optimization and analysis of probabilistic caching in N-tier heterogeneous networks. *IEEE Transactoins on Wireless Communications*, 17(2):1283–1297, 2018.
- [41] Dong Liu, Binqiang Chen, Chenyang Yang, and Andreas F. Molisch. Caching at the wireless edge: design aspects, challenges, and future directions. *IEEE Communications Magazine*, 54(9):22–28, September 2016.
- [42] Dong Liu and Chenyang Yang. Optimal content placement for offloading in cache-enabled heterogeneous wireless networks. In *IEEE Global Communications Conference (GLOBECOM)*, pages 1–6, 2016.
- [43] Dong Liu and Chenyang Yang. Caching policy toward maximal success probability and area spectral efficiency of cache-enabled HetNets. *IEEE Transactoins on Communications*, 65(6):2699–2714, 2017.
- [44] Bojie Lv, Lexiang Huang, and Rui Wang. Joint downlink scheduling for file placement and delivery in cache-assisted wireless networks with finite file lifetime. *IEEE Transactoins on Communications*, 67(6):4177–4192, 2019.

- [45] Mohammad Ali Maddah-Ali and Urs Niesen. Fundamental limits of caching. *IEEE Transactions on Information Theory*, 60(5):2856—2867, May 2014.
- [46] Mohammad Ali Maddah-Ali and Urs Niesen. Decentralized coded caching attains order-optimal memory-rate tradeoff. *IEEE/ACM Transactions on Networking*, 23(4):1029–1040, 2015.
- [47] Leonardo Militano, Massimo Condoluci, Giuseppe Araniti, Antonella Molinaro, Antonio Iera, and Gabriel-Miro Muntean. Single frequency-based device-to-device-enhanced video delivery for evolved multimedia broadcast and multicast services. *IEEE Transactions on Broadcasting*, 61(2):263–278, June 2015.
- [48] Mark P. Mills. The cloud begins with coal. *White paper*, Aug. 2013.
- [49] Urs Niesen and Mohammad Ali Maddah-Ali. Coded caching with nonuniform demands. In *2014 IEEE Conference on Computer Communications Workshops (INFOCOM)*, pages 221–226, 2014.
- [50] Urs Niesen, Devavrat Shah, and Gregory Wornell. Caching in wireless networks. pages 2111–2115, 2009.
- [51] Santiago Paternain, Manfred Morari, and Alejandro Ribeiro. Real-time model predictive control based on prediction-correction algorithms. In *2019 IEEE 58th Conference on Decision and Control (CDC)*, pages 5285–5291, 2019.
- [52] Ramtin Pedarsani, Mohammad Ali Maddah-Ali, and Urs Niesen. Online coded caching. *IEEE/ACM Transactions on Networking*, 24(2):836–845, April 2016.
- [53] Xi Peng, Yuanming Shi, Jun Zhang, and Khaled B. Letaief. Layered group sparse beamforming for cache-enabled green wireless networks. *IEEE Transactions on Communications*, 65(12):5589–5603, 2017.
- [54] Robert Pepper. Cisco visual networking index (VNI) global mobile data traffic forecast update. *Cisco, Technology Report*, Feb. 2013.
- [55] Helen Roeth and Leena Woheck. ICTs and climate change mitigation in emerging economies. Technical report (TR), 2011.
- [56] Letian Rong, Olfa Ben Haddada, and Salah-Eddine Elayoubi. Analytical analysis of the coverage of a MBSFN OFDMA network. In *IEEE Glob. Commun. Conf. (GLOBECOM)*, pages 1–5, 2008.
- [57] Alireza Sadeghi, Fatemeh Sheikholeslami, and Georgios B. Giannakis. Optimal and scalable caching for 5G using reinforcement learning of space-time popularities. *IEEE Journal of Selected Topics in Signal Processing*, 12(1):180–190, Feb 2018.
- [58] Hikmet Sari, Georges Karam, and Isabelle Jeanclaude. Transmission techniques for digital terrestrial TV broadcasting. *IEEE Communications Magazine*, 33(2):100–109, February 1995.
- [59] Berksan Serbetci and Jasper Goseling. On optimal geographical caching in heterogeneous cellular networks. In *IEEE Wireless Communications and Networking Conference (WCNC)*, pages 1–6, March. 2017.
- [60] Berksan Serbetci and Jasper Goseling. Optimal geographical caching in heterogeneous cellular networks with non-homogeneous helpers. preprint ArXiv 1710.09626v3, 2019.

- [61] Andrea Simonetto, Emiliano Dall’Anese, Santiago Paternain, Geert Leus, and Georgios B. Giannakis. Time-varying convex optimization: Time-structured algorithms and applications. 2020.
- [62] Heidi Steendam and Marc Moeneclaey. Analysis and optimization of the performance of OFDM on frequency-selective time-selective fading channels. *IEEE Transactions on Communications*, 47(12):1811–1819, 1999.
- [63] Weiqi Sun, Yong Li, Chunjing Hu, and Mugen Peng. Joint optimization of cache placement and bandwidth allocation in heterogeneous networks. *IEEE Access*, 6:37250–37260, 2018.
- [64] Richard S. Sutton and Andrew G. Barto. *Reinforcement Learning: An Introduction*. Cambridge, MA: MIT Press, 1998.
- [65] Meixia Tao, Erkai Chen, Hao Zhou, and Wei Yu. Content-centric sparse multicast beamforming for cache-enabled cloud RAN. *IEEE Transactions on Wireless Communications*, 15(9):6118–6131, Sep. 2016.
- [66] Zitian Wang, Zhehan Cao, Ying Cui, and Yang Yang. Joint and competitive caching designs in large-scale multi-tier wireless multicasting networks. In *IEEE Global Communications Conference (GLOBECOM)*, volume abs/1706.07903, pages 1–7, 2017.
- [67] Juan Wen, Kaibin Huang, Sheng Yang, and Victor O. K. Li. Cache-enabled heterogeneous cellular networks: Optimal tier-level content placement. *IEEE Transactions on Wireless Communications*, 16(9):5939–5952, 2017.
- [68] Franciscus X. A. Wibowo, Arya A. P. Bangun, Adit Kurniawan, and Hendrawan. Multimedia broadcast multicast service over single frequency network (MBSFN) in LTE based femtocell. In *International Conference on Electrical Engineering and Informatics (ICEEI)*, pages 1–5, July 2011.
- [69] Ronald J. Williams and Jing Peng. Function optimization using connectionist reinforcement learning algorithms. *Connection Science*, 3(3):241–268, 1991.
- [70] Jiajun Wu, Binqiang Chen, Chenyang Yang, and Qi Li. Caching and bandwidth allocation policy optimization in heterogeneous networks. In *IEEE International Symposium on Personal, Indoor and Mobile Radio Communications PIMRC*, pages 1–6, October 2017.
- [71] Jiajun Wu, Chenyang Yang, and Binqiang Chen. Proactive caching and bandwidth allocation in heterogeneous networks by learning from historical numbers of requests. *IEEE Transactions on Communications*, 68(7):4394–4410, 2020.
- [72] Xianzhe Xu and Meixia Tao. Analysis and optimization of probabilistic caching in multi-antenna small-cell networks. In *IEEE Global Communications Conference (GLOBECOM)*, pages 1–6, 2017.
- [73] Xianzhe Xu and Meixia Tao. Modeling, analysis, and optimization of caching in multi-antenna small-cell networks. *IEEE Transactions on Wireless Communications*, 18(11):5454–5469, 2019.
- [74] Jie Yan, Yanxiang Jiang, Fuchun Zheng, F. Richard Yu, Xiqi Gao, and Xiaohu You. Distributed edge caching via reinforcement learning in fog radio access networks. In *IEEE Vehicular Technology Conference (VTC)*, pages 1–6, 2019.
- [75] Chencheng Ye, Ying Cui, Yang Yang, and Rui Wang. Optimal caching designs for perfect, imperfect, and unknown file popularity distributions in large-scale multi-tier wireless networks. *IEEE Transactions on Communications*, 67(9):6612–6625, 2019.

- [76] Seung Min Yu and Seong-Lyun Kim. Downlink capacity and base station density in cellular networks. In *International Symposium and Workshops on Modeling and Optimization in Mobile, Ad Hoc and Wireless Networks (WiOpt)*, pages 119–124, 2013.
- [77] Qingtian Zeng, Qiang Sun, Geng Chen, Hua Duan, Chao Li, and Ge Song. Traffic prediction of wireless cellular networks based on deep transfer learning and cross-domain data. *IEEE Access*, 8:172387–172397, 2020.
- [78] Nan Zhao, Fen Cheng, Fei Richard Yu, Jie Tang, Yunfei Chen, Guan Gui, and Hikmet Sari. Caching UAV assisted secure transmission in hyperdense networks based on interference alignment. *IEEE Transactions on Communications*, 66(5):2281–2294, 2018.
- [79] Shan Zhong and Xiaodong Wang. Joint multicast and unicast beamforming for coded caching. *IEEE Trans. on Commun.*, 66(8):3354–3367, 2018.
- [80] Fasheng Zhou, Lisheng Fan, Ning Wang, Gaoyong Luo, Jie Tang, and Wei Chen. A cache-aided communication scheme for downlink coordinated multi-point transmission. *IEEE Access*, 6:1416–1427, December 2018.

Errata

Publication I:

In Corollary 1, $\operatorname{erfc}\left(\frac{\pi^2 \lambda q_n}{4\sqrt{2\eta_n}}\right)$ should be replaced by $\operatorname{erfc}\left(\frac{\pi^2 \lambda q_n}{4\sqrt{\eta_n}}\right)$.

In Equation (12), $\operatorname{erfc}\left(\frac{\pi^2 \lambda_{\text{eff}} p_n}{4\sqrt{2\eta_n}}\right)$ should be replaced by $\operatorname{erfc}\left(\frac{\pi^2 \lambda_{\text{eff}} p_n}{4\sqrt{\eta_n}}\right)$.

In Equation (13), $\operatorname{erfc}\left(\frac{\pi^2 \lambda/v}{4\sqrt{2\eta_v}}\right)$ should be replaced by $\operatorname{erfc}\left(\frac{\pi^2 \lambda/v}{4\sqrt{\eta_v}}\right)$.



ISBN 978-952-64-1600-7 (printed)

ISBN 978-952-64-1601-4 (pdf)

ISSN 1799-4934 (printed)

ISSN 1799-4942 (pdf)

Aalto University

School of Electrical Engineering

Department of Information and Communications Engineering

www.aalto.fi

**BUSINESS +
ECONOMY**

**ART +
DESIGN +
ARCHITECTURE**

**SCIENCE +
TECHNOLOGY**

CROSSOVER

**DOCTORAL
THESES**